Calcolo manuscript No.
(will be inserted by the editor)

Reduced Basis Approximation and A Posteriori Error Estimation for the Time-Dependent Viscous Burgers' Equation

Ngoc-Cuong Nguyen[1], **Gianluigi Rozza**[1,⋆], **Anthony T. Patera**[1]

Massachusetts Institute of Technology, Department of Mechanical Engineering, Room 3-264, 77 Massachusetts Avenue, Cambridge MA, 02142-4307, USA; Email addresses: cuongng@mit.edu, rozza@mit.edu, patera@mit.edu

Received: 17 June 2008 / Revised version: 2 April 2009

Abstract. In this paper we present rigorous *a posteriori* L^2 error bounds for reduced basis approximations of the unsteady viscous Burgers' equation in one space dimension. The *a posteriori* error estimator, derived from standard analysis of the error–residual equation, comprises two key ingredients — both of which admit efficient Offline–Online treatment: the first is a sum over timesteps of the square of the dual norm of the residual; the second is an accurate upper bound (computed by the Successive Constraint Method) for the exponential–in–time stability factor. These error bounds serve both Offline for construction of the reduced basis space by a new POD–Greedy procedure and Online for verification of fidelity. The *a posteriori* error bounds are practicable for final times (measured in convective units) $T \approx O(1)$ and Reynolds numbers $\nu^{-1} \gg 1$; we present numerical results for a (stationary) steepening front for $T = 2$ and $1 \leq \nu^{-1} \leq 200$.

This work was supported by AFOSR Grants FA9550-05-1-0114 and FA-9550-07-1-0425 and the Singapore-MIT Alliance. We acknowledge many helpful discussions with Professor Yvon Maday of University of Paris VI and Dr. Paul Fischer of Argonne National Laboratory and University of Chicago.

⋆ *Corresponding Author*; Present Address: Ecole Polytechnique Fédérale de Lausanne, Institute of Analysis and Scientific Computing, Station 8-MA, CH-1015 Lausanne, Switzerland. Email address: gianluigi.rozza@epfl.ch

1. Introduction

The reduced basis method and related model–reduction approaches are well developed for linear parametrized parabolic partial differential equations [10,12,15,30,34]. The reduced basis approach — built upon an underlying "truth" finite element discretization which we wish to accelerate — can provide both very reliable results *and* very rapid response in the real–time and many–query contexts. The former (reliability) is ensured by rigorous *a posteriori* bounds for the error in the reduced basis approximation relative to the truth finite element discretization: we provide estimators for the field variable in the relevant norms as well as for any particular scalar output(s) of interest. The latter (rapid response) is ensured by an Offline–Online computational strategy that minimizes marginal cost: in an expensive Offline stage we prepare a very small reduced basis "database"; in the Online stage, for each new parameter value of interest, we rapidly evaluate both the output of interest and the associated *a posteriori* error bound — in complexity *independent* of the dimensionality of the truth finite element approximation space.

However, in the nonlinear case there are still many open research issues. We shall focus in this paper on the development of rigorous *a posteriori* error bounds for the one–dimensional parametrized unsteady viscous Burgers' equation; the Burgers' equation is of interest primarily as a model for the unsteady incompressible Navier–Stokes equations, the extension to which is considered in subsequent papers [27,26]. There are examples of rigorous reduced basis *a posteriori* error bounds for the *steady* Burgers' [37] and incompressible Navier–Stokes [28,36] equations; the new contribution of the current paper is treatment of the unsteady — parabolic — case. Although there are many examples of reduced order models for the unsteady incompressible Navier–Stokes equations [5,7,9,13,14,17–21], none is endowed with rigorous *a posteriori* error bounds.

The unsteady viscous Burgers' equation, like the unsteady incompressible Navier–Stokes system, appears computationally simple: a quadratic nonlinearity that admits standard Galerkin treatment. (Note for higher–order and non–polynomial nonlinearities more sophisticated re-

duced basis approximations must be considered [3,6,11,32] that in turn introduce both numerical and theoretical complications. The results of the current paper do not directly extend to these more difficult cases.) However, in the interesting case of small viscosity the unsteady viscous Burgers' equation, like the unsteady incompressible Navier–Stokes system [8,22], is in fact computationally difficult: exponential instability compromises *a priori* and *a posteriori* error estimates — any *useful* bounds are perforce limited to modest (final) times and modest Reynolds numbers. (More precisely, stability considerations will limit the product of the final time and the Reynolds number.)

The approach developed in this paper does not eliminate the exponential growth in time. (In some cases [22] it may be possible to demonstrate algebraic growth in time; however, more generally — most simply, linearly unstable flows — we must admit exponential sensitivity to disturbances.) Rather we develop a procedure, within the reduced basis context, for the calculation of a more accurate estimate for the stability factor which reflects the full spatial and temporal structure of the solution. The resulting error bounds, though certainly still pessimistic, are practicable for final times (measured in convective units) $T \approx O(1)$ and Reynolds numbers $\nu^{-1} \gg 1$; we demonstrate the relevance of our bounds to fluid dynamically interesting contexts — response - to - disturbance and bifurcation analyses — in [27,26]. The error bounds serve not only for certification, but also for efficient construction of rapidly convergent reduced basis approximations.

In Section 2 we introduce the reduced basis (RB) approximation for the unsteady viscous Burgers' equation. In Section 3.1 we develop the associated *a posteriori* error bounds; in Section 3.2 we describe the formulation and calculation of the stability growth factor by the Successive Constraint Method (SCM). In Section 4.1 we summarize the Offline–Online (or "Construction-Evaluation") computational strategy for efficient evaluation of the reduced basis prediction and associated *a posteriori* error bound; in Sections 4.2 and 4.3 we describe POD–Greedy$_{\mathrm{RB}}$ and Greedy$_{\mathrm{SCM}}$ sampling approaches for construction of the reduced basis space and the SCM

parameter sample, respectively. Finally, in Section 5 we present numerical results — which are particularly important in the present context since the stability factors, and hence the utility of the bounds, can only be determined *in situ*.

As already indicated, in this paper we address for the first time rigorous reduced basis *a posteriori* error bounds for the unsteady viscous Burgers' equation: our emphasis is on the requisite theoretical and computational innovations. This new material includes the development of the error bound for quadratically nonlinear parabolic equations; the adaptation of the Successive Constraint Method (SCM) procedure to the calculation of solution– and time–dependent stability factors; a new POD–Greedy procedure, based on an earlier proposal in [15], for time-parameter sampling; and finally numerical results that demonstrate the practical relevance of the proposed approach. Note, however, that for completeness we do include in this paper a summary of some earlier work: a brief description of the Offline–Online approach to evaluation of the dual norm of the residual [28,36]; and a short summary of the Successive Constraint Method (SCM) [16,35].

2. Reduced Basis Approximation

To begin, we introduce the domain $\Omega =]0,1[$ and the space $X = H_0^1(\Omega)$, where $H_0^1(\Omega) = \{v \in H^1(\Omega) \,|\, v(0) = v(1) = 0\}$, $H^1(\Omega) = \{v \in L^2(\Omega) \,|\, v_x \in L^2(\Omega)\}$, and $L^2(\Omega) = \{v \,\text{measurable} \,|\, \int_\Omega v^2 < \infty\}$. We further define the X inner product and norm as $(w,v)_X = \int_\Omega w_x v_x$ and $\|w\|_X = \sqrt{(w,w)_X}$, respectively, and the $L^2(\Omega)$ inner product and norm as $(w,v) \equiv \int_\Omega wv$ and $\|w\| \equiv \sqrt{(w,v)}$, respectively. Finally, we introduce the closed parameter (viscosity) domain $\mathcal{D} \equiv [\nu_{\min}, \nu_{\max}]$ with $0 < \nu_{\min} < \nu_{\max}$.

We next introduce $L^2(\Omega)$–continuous linear functionals f and ℓ. Then, given $\nu \in \mathcal{D}$, $\mathcal{U}(\nu) \in L^2(0,T;X) \cap C^0([0,T];L^2(\Omega))$ [33] satisfies

$$\frac{d}{dt}(\mathcal{U}(t;\nu),v) + c(\mathcal{U}(t;\nu),\mathcal{U}(t;\nu),v) + \nu a(\mathcal{U}(t;\nu),v) = f(v), \quad \forall v \in X, \tag{1}$$

with initial condition $\mathcal{U}(t=0;\nu)=0$. We subsequently evaluate our "output of interest": for all times $t \in [0,T]$,

$$\mathcal{S}(t;\nu) = \ell(\mathcal{U}(t;\nu)). \tag{2}$$

Here T is the final time, $C^0(I)$ is the space of continuous functions over the interval I, ν denotes the viscosity — we shall sometimes refer to ν^{-1} as the Reynolds number — and

$$\begin{aligned} c(w,z,v) &= -\frac{1}{2}\int_\Omega wzv_x, \\ a(w,v) &= \int_\Omega w_x v_x, \end{aligned} \tag{3}$$

are the convective trilinear and viscous bilinear forms, respectively. Equations (1) and (3) represent the standard unsteady viscous Burgers' equation in one space dimension [25]; in our numerical experiments we shall choose $f(v) = \ell(v) = \int_\Omega v$, as we discuss in greater detail in Section 5.

We next introduce the time–discrete Burgers' equation. Towards that end, we first divide the time interval $[0,T]$ into K subintervals of equal length $\Delta t = T/K$; we then define $t^k \equiv k\Delta t$, $0 \le k \le K$. Given $\nu \in \mathcal{D}$, we now look for $u^k(\nu) \in X, 0 \le k \le K$, such that $u^0(\nu) = 0$ and

$$\frac{1}{\Delta t}(u^k(\nu) - u^{k-1}(\nu), v) + c(u^k(\nu), u^k(\nu), v) + \nu a(u^k(\nu), v) = f(v), \quad \forall v \in X, \tag{4}$$

for $1 \le k \le K$. We then evaluate the associated output: for $0 \le k \le K$,

$$s^k(\nu) = \ell(u^k(\nu)). \tag{5}$$

We shall sometimes denote $u^k(\nu)$ as $u(t^k;\nu)$ and $s^k(\nu)$ as $s(t^k;\nu)$ to more clearly identify the discrete time levels. Equation (4) – Euler Backward discretization of (1) — shall be our point of departure: we shall presume that Δt is chosen sufficiently small that $u^k(\nu) = u(t^k;\nu)$ and $s^k(\nu) = s(t^k;\nu)$ are effectively indistinguishable from $\mathcal{U}(t^k;\nu)$ and $\mathcal{S}(t^k;\nu)$, respectively. For our purposes, the timestep Δt is fixed; we do not consider $\Delta t \to 0$. (The development readily

extends to Crank-Nicolson discretization; for purposes of exposition, we consider the simple Euler Backward approach.)

We next introduce a Galerkin finite element "truth" spatial discretization of our (already time–discrete) equation (4). We denote by $X^{\mathcal{N}}$ the standard conforming linear finite element space over a uniform "triangulation" of Ω comprising $\mathcal{N}+1$ elements each of length $1/(\mathcal{N}+1)$; note that $X^{\mathcal{N}}$ is of dimension $\mathcal{N}$. Then, given $\nu \in \mathcal{D}$, we look for $u^{\mathcal{N}\,k}(\nu) \in X^{\mathcal{N}}, 0 \le k \le K$, such that $u^{\mathcal{N}\,0}(\nu) = 0$ and

$$\frac{1}{\Delta t}(u^{\mathcal{N}\,k}(\nu) - u^{\mathcal{N}\,k-1}(\nu), v) + c(u^{\mathcal{N}\,k}(\nu), u^{\mathcal{N}\,k}(\nu), v) + \nu a(u^{\mathcal{N}\,k}(\nu), v) = f(v), \quad \forall v \in X^{\mathcal{N}}, \quad (6)$$

for $1 \le k \le K$. We then evaluate the associated output: for $0 \le k \le K$,

$$s^{\mathcal{N}\,k}(\nu) = \ell(u^{\mathcal{N}\,k}(\nu)). \quad (7)$$

We shall build our reduced basis approximation upon the "truth" discretization (6), and we shall measure the error in our reduced basis prediction relative to $u^{\mathcal{N}\,k}(\nu) \equiv u^{\mathcal{N}}(t^k;\nu)$ and $s^{\mathcal{N}\,k}(\nu) \equiv s^{\mathcal{N}}(t^k;\nu)$. (As we shall observe, the Online cost (and stability) of the reduced basis evaluations shall be independent of $\mathcal{N}$: we may thus choose $\mathcal{N}$ conservatively.)

Finally, we introduce the reduced basis approximation. Given a set of mutually $(\cdot,\cdot)_X$–orthogonal basis functions $\xi_n \in X^{\mathcal{N}}, 1 \le n \le N_{\max}$, the hierarchical reduced basis spaces are given by

$$X_N \equiv \text{span}\,\{\xi_n, 1 \le n \le N\}, \quad 1 \le N \le N_{\max}. \quad (8)$$

The reduced basis approximation to $u^{\mathcal{N}\,k}(\nu) \in X^{\mathcal{N}}$, $u_N^k(\nu) \in X_N$, shall be expressed as

$$u_N^k(\nu) = \sum_{n=1}^{N} \omega_{N\,n}^k(\nu)\xi_n. \quad (9)$$

The spaces $X_N \in X^{\mathcal{N}}, 1 \le N \le N_{\max}$, and basis functions $\xi_n, 1 \le N \le N_{\max}$, will be generated by a POD–Greedy$_{\text{RB}}$ sampling procedure which combines spatial snapshots in time and viscosity

— $u^{\mathcal{N}\,k}(\nu)$ — in an optimal fashion. The POD–Greedy$_{\rm RB}$ will normalize the basis functions such that $\|\xi_n\|_X \to 0$ exponentially fast as n increases; we shall observe $\omega^k_{N\,n}(\nu) \sim O(1), 1 \le n \le N$ — consistent with rapid convergence of the reduced basis approximation.

We now introduce the Galerkin reduced basis approximation. Given $\nu \in \mathcal{D}$, we look for $u^k_N(\nu) \in X_N, 0 \le k \le K$, such that $u^0_N(\nu) = 0$ and

$$\frac{1}{\Delta t}(u^k_N(\nu) - u^{k-1}_N(\nu), v) + c(u^k_N(\nu), u^k_N(\nu), v) + \nu a(u^k_N(\nu), v) = f(v), \quad \forall v \in X_N, \tag{10}$$

for $1 \le k \le K$. We then evaluate the associated output: for $0 \le k \le K$,

$$s^k_N(\nu) = \ell(u^k_N(\nu)). \tag{11}$$

(In Section 4, we shall develop the algebraic equations associated with (10)-(11).) We shall sometimes denote $u^k_N(\nu)$ as $u_N(t^k;\nu)$ and $s^k_N(\nu)$ as $s_N(t^k;\nu)$ to more clearly identify the discrete time levels. In fact all the reduced basis quantities should bear a $\mathcal{N}$ — $X^{\mathcal{N}}_N, u^{\mathcal{N}\,k}_N(\nu), s^{\mathcal{N}\,k}_N(\nu)$ — since the reduced basis approximation is defined in terms of a particular truth discretization: for clarity of exposition, we shall typically suppress the "truth" superscript; however, we shall insist upon stability/uniformity of our reduced basis approximation as $\mathcal{N} \to \infty$.

The goal of the reduced basis approximation is simple: dimension reduction — $N \ll \mathcal{N}$ — and associated computational economies. (Note however that there is no "reduction in time": the reduced basis approximation inherits the fixed Δt of the truth approximation.) Obviously, for the Burgers' equation in one space dimension, there is not much room for significant economies; however, in higher spatial dimensions, (Online) reduced basis evaluation is typically several orders of magnitude less expensive than the classical finite element approach [31,35,27,26].

3. *A Posteriori* Error Bound

3.1. L^2 Error Bound

In this section we aim to develop an *a posteriori* bound $\Delta_N^k(\nu) \equiv \Delta_N(t^k;\nu), 1 \le k \le K$, for the L^2 error in the solution such that

$$\|u^{\mathcal{N}\,k}(\nu) - u_N^k(\nu)\| \le \Delta_N^k(\nu), \quad 1 \le k \le K, \quad \forall \nu \in \mathcal{D}, \tag{12}$$

for any $N = 1, \ldots, N_{\max}$. (We note that L^2 estimates for the *linear* parabolic case are considered in [15].) Since the linear output functional ℓ is in $L^2(\Omega)$, the error in the output satisfies

$$|s^{\mathcal{N}\,k}(\nu) - s_N^k(\nu)| \le \Delta_N^{s\,k}(\nu), \quad 1 \le k \le K, \, \forall \nu \in \mathcal{D}, \tag{13}$$

where $\Delta_N^{s\,k}(\nu)$, which we shall denote the "output error bound," is given by

$$\Delta_N^{s\,k}(\nu) = \left(\sup_{v \in X^{\mathcal{N}}} \frac{\ell(v)}{\|v\|} \right) \Delta_N^k(\nu). \tag{14}$$

We introduce the effectivities associated with these error estimates as

$$\eta_N(t^k;\nu) = \frac{\Delta_N^k(\nu)}{\|u^{\mathcal{N}k}(\nu) - u_N^k(\nu)\|} \quad \text{and} \quad \eta_N^s(t^k;\nu) = \frac{\Delta_N^{s\,k}(\nu)}{|s^{\mathcal{N}\,k}(\nu) - s_N^k(\nu)|}. \tag{15}$$

Clearly, the effectivities are a measure of the quality of the proposed estimator: for rigor, we shall insist upon effectivities ≥ 1; for sharpness, we desire effectivities as close to unity as possible.

There are two main components to our error bounds. The first component is the dual norm of the residual

$$\varepsilon_N(t^k;\nu) = \sup_{v \in X^{\mathcal{N}}} \frac{r_N(v;t^k;\nu)}{\|v\|_X}, \quad 1 \le k \le K, \tag{16}$$

where $r_N(v;t^k;\nu)$ is the residual associated with the reduced basis approximation (10)

$$r_N(v;t^k;\nu) = f(v) - \frac{1}{\Delta t}\big(u_N^k(\nu) - u_N^{k-1}(\nu), v\big) \\ - c\big(u_N^k(\nu), u_N^k(\nu), v\big) - \nu a\big(u_N^k(\nu), v\big), \quad \forall v \in X^{\mathcal{N}}, \quad 1 \le k \le K. \quad (17)$$

Note the dual norm is defined over $X^{\mathcal{N}}$, and not X, since we measure our reduced basis error relative to the truth finite element discretization.

The second component is a lower bound

$$\rho_N^{\mathrm{LB}}(t^k;\nu) \le \rho_N(t^k;\nu), \quad 1 \le k \le K, \quad \forall \nu \in \mathcal{D}, \quad (18)$$

for the stability constant $\rho_N(t^k;\nu)$ defined as

$$\rho_N(t^k;\nu) = \inf_{v \in X^{\mathcal{N}}} \frac{4c\big(u_N^k(\nu), v, v\big) + \nu a(v,v)}{\|v\|^2}, \quad 1 \le k \le K, \quad \forall \nu \in \mathcal{D}; \quad (19)$$

efficient calculation of $\rho_N^{\mathrm{LB}}(t^k;\nu)$ is the topic of section 3.2. The stability constant (19) — negative values shall result in *growth* — is closely related to the absolute (monotonic decay) criterion of hydrodynamic stability theory [23].

We can demonstrate

Proposition 1. *There exists a positive constant* $\underline{C}$ *independent of* ν *such that*

$$\rho_N(t^k;\nu) \ge -\underline{C}\frac{\|u_N^k(\nu)\|^4}{\nu^3}, \quad 1 \le k \le K, \quad (20)$$

for $\rho_N(t^k;\nu)$ *defined in* (19).

Proof. We first observe that, for any $v \in X$,

$$\begin{aligned} |4c(u_N^k(\nu), v, v)| =& 2 \left\| \int_0^1 u_N^k(\nu) v v_x dx \right\| \\ \leq& 2 \|u_N^k(\nu)\| \|v\|_{L^\infty(\Omega)} \|v\|_X \\ \leq& 4 \|u_N^k(\nu)\| \|v\|^{1/2} \|v\|_X^{1/2} \|v\|_X \end{aligned} \tag{21}$$

by the L^∞-H^1 embedding (which perforce restricts our arguments to one space dimension), the Cauchy-Schwarz inequality, and a Gagliardi–Nirenberg inequality. We then apply the Young inequality twice to obtain

$$\begin{aligned} 4 \|v\|^{1/2} \|v\|_X^{3/2} \|u_N^k(\nu)\| \leq& 2 \left(\delta \|v\| + \frac{\|v\|_X^3}{\delta} \right) \|u_N^k(\nu)\| \\ \leq& \left(\kappa \|v\|^2 \|u_N^k(\nu)\|^2 + \frac{\delta^2}{\kappa} \right) + \frac{2\|v\|_X^3 \|u_N^k(\nu)\|}{\delta}, \quad \forall v \in X, \end{aligned} \tag{22}$$

for any positive δ and κ. We now choose $\delta = \frac{4\|u_N^k(\nu)\| \|v\|_X}{\nu}$ and $\kappa = \frac{32\|u_N^k(\nu)\|^2}{\nu^3}$ to obtain for all $v \in X$ (and hence all $v \in X^{\mathcal{N}} \subset X$)

$$|4c(u_N^k(\nu), v, v)| \leq 32 \frac{\|u_N^k(\nu)\|^4 \|v\|^2}{\nu^3} + \nu \|v\|_X^2. \tag{23}$$

Therefore, we have

$$\rho_N(t^k; \nu) \geq -32 \frac{\|u_N^k(\nu)\|^4}{\nu^3}, \quad 1 \leq k \leq K, \tag{24}$$

which proves the desired result for $\underline{C} = 32$. □

(Note that $\|u_N^k(\nu)\|$ may be bounded in terms of f, ν, and T, which in turn provides a lower bound for $\rho_N(t^k; \nu)$ which is independent of $\mathcal{N}$.) This extremely pessimistic bound is of course of very little comfort or utility; in our actual estimation procedure for $\rho_N(t^k; \nu)$, described in the next section, we reflect the full temporal–spatial structure of $u_N^k(\nu), 1 \leq k \leq K$, and obtain more meaningful and useful lower bounds.

We can now define our error bound $\Delta_N^k(\nu), 1 \le k \le K$, in terms of the dual norm of the residual and the lower bound for the stability constant. We first define

$$\Delta t_N^*(\nu) = \frac{1}{2|\min(0, \min_{1\le k\le K} \rho_N^{\rm LB}(t^k;\nu))|}. \tag{25}$$

Then, for $\Delta t < \Delta t_N^*(\nu)$, which ensures $1 + \Delta t \rho_N^{\rm LB}(t^k;\nu) > 0, 1 \le k \le K$, we define our *a posteriori* error bound as

$$\Delta_N^k(\nu) = \sqrt{\frac{\frac{\Delta t}{\nu}\sum_{m=1}^k \left(\varepsilon_N^2(t^m;\nu)\prod_{j=1}^{m-1}\left(1+\Delta t\,\rho_N^{\rm LB}(t^j;\nu)\right)\right)}{\prod_{m=1}^k\left(1+\Delta t\,\rho_N^{\rm LB}(t^m;\nu)\right)}} \quad 1 \le k \le K. \tag{26}$$

Note (26) is the Euler Backward version of the classical continuous–time exponential result. (The particular fashion in which $\rho_N^{\rm LB}(t^j;\nu)$ appears in our bound — in particular, as an integral in time — is important in the generalization of Proposition 1 to the case of higher space dimensions.)

For ν sufficiently large (Reynolds sufficiently small), $\rho_N(t^k;\nu)$ will be uniformly positive and hence error growth will be controlled; in this case, we can consider rather large times — effectively reaching steady or (say) steady-periodic states. However, for smaller ν, $\rho_N(t^k;\nu)$ will certainly be negative and hence the error bound (26) will grow exponentially in time; in this case, we will be practically limited to modest final times — the smaller the ν, the smaller the practicable final time T. In fact, the actual limitations are less severe than might be anticipated: we quantify the restrictions for a particular Burgers' example in Section 5, and for several Navier-Stokes examples in [27,26]. (Clearly, the $\nu^{-1/2}$ prefactor in the error bound (26) is also less than welcome; future work will consider different norms to attenuate this effect.)

To close this section we prove (12) for our bound of (26) by appropriate modification of classical procedures [33]:

Proposition 2. *For given $\nu \in \mathcal{D}$, $\Delta t < \Delta t_N^*(\nu)$ of (25), and error bound $\Delta_N^k(\nu)$ defined in* (26)*, the error estimate* (12) *holds for any $N \in [1, N_{\max}]$.*

Proof. We note from (6) and (17) that the error $e^m(\nu) \equiv u^{\mathcal{N}\,m}(\nu) - u_N^m(\nu)$ satisfies

$$\frac{1}{\Delta t}\big(e^m(\nu) - e^{m-1}(\nu), v\big) + c\big(u^{\mathcal{N}\,m}(\nu), u^{\mathcal{N}\,m}(\nu), v\big) - c\big(u_N^m(\nu), u_N^m(\nu), v\big) + \nu a\big(e^m(\nu), v\big) = r_N(v; t^m; \nu), \quad \forall v \in X^{\mathcal{N}}. \quad (27)$$

From trilinearity, and symmetry in the first two arguments, of the form c in (3) we can derive the following equality

$$c\big(u^{\mathcal{N}\,m}(\nu), u^{\mathcal{N}\,m}(\nu), v\big) - c\big(u_N^m(\nu), u_N^m(\nu), v\big) = c\big(e^m(\nu), e^m(\nu), v\big) + 2c\big(u_N^m(\nu), e^m(\nu), v\big), \quad \forall v \in X^{\mathcal{N}}. \quad (28)$$

It thus follows that

$$\frac{1}{\Delta t}\big(e^m(\nu) - e^{m-1}(\nu)(\nu), v\big) + c\big(e^m(\nu), e^m(\nu), v\big) + 2c\big(u_N^m(\nu), e^m(\nu), v\big) + \nu a\big(e^m(\nu), v\big) = r_N(v; t^m; \nu), \quad \forall v \in X^{\mathcal{N}}. \quad (29)$$

We now choose $v = e^m(\nu)$ in (29) and invoke (16) to find

$$\frac{1}{\Delta t}\big(e^m(\nu) - e^{m-1}(\nu), e^m(\nu)\big) + c\big(e^m(\nu), e^m(\nu), e^m(\nu)\big) + 2c\big(u_N^m(\nu), e^m(\nu), e^m(\nu)\big) + \nu a\big(e^m(\nu), e^m(\nu)\big) \le \varepsilon_N(t^m; \nu)\|e^m(\nu)\|_X. \quad (30)$$

Application of Young's inequality, $2AB \le \frac{1}{\epsilon}A^2 + \epsilon B^2, \forall \epsilon > 0$, yields (for $\epsilon = \nu$)

$$\begin{aligned}\varepsilon_N(t^m; \nu)\|e^m(\nu)\|_X &\le \frac{1}{2}\Big(\frac{1}{\nu}\varepsilon_N^2(t^m; \nu) + \nu\|e^m(\nu)\|_X^2\Big) \\ &= \frac{1}{2}\Big(\frac{1}{\nu}\varepsilon_N^2(t^m; \nu) + \nu a\big(e^m(\nu), e^m(\nu)\big)\Big). \end{aligned} \quad (31)$$

We now use $\|e^m(\nu) - e^{m-1}(\nu)\|^2 > 0$ and the equality

$$c\big(e^m(\nu), e^m(\nu), e^m(\nu)\big) = -\frac{1}{6}\int_0^1 \frac{\partial e^3(t^m;\nu)}{\partial x} = 0 \tag{32}$$

to reduce (30) to

$$\frac{1}{\Delta t}\Big(\big(e^m(\nu), e^m(\nu)\big) - \big(e^{m-1}(\nu), e^{m-1}(\nu)\big)\Big) + 4c\big(u_N^m(\nu), e^m(\nu), e^m(\nu)\big) + \nu a\big(e^m(\nu), e^m(\nu)\big) \leq \frac{1}{\nu}\varepsilon_N^2(t^m;\nu). \tag{33}$$

Hence, from (33) and (18)-(19) we obtain

$$\Big(1 + \Delta t\, \rho_N^{\mathrm{LB}}(t^m;\nu)\Big)\big(e^m(\nu), e^m(\nu)\big) - \big(e^{m-1}(\nu), e^{m-1}(\nu)\big) \leq \frac{\Delta t}{\nu}\varepsilon_N^2(t^m;\nu). \tag{34}$$

We now multiply by (the positive quantity, given our hypothesis on Δt) $\prod_{j=1}^{m-1}\big(1 + \Delta t\, \rho_N^{\mathrm{LB}}(t^j;\nu)\big)$ on both sides of (34) to obtain

$$\big(e^m(\nu), e^m(\nu)\big)\prod_{j=1}^{m}\big(1 + \Delta t\, \rho_N^{\mathrm{LB}}(t^j;\nu)\big) - \big(e^{m-1}(\nu), e^{m-1}(\nu)\big)\prod_{j=1}^{m-1}\big(1 + \Delta t\, \rho_N^{\mathrm{LB}}(t^j;\nu)\big) \leq \frac{\Delta t}{\nu}\varepsilon_N^2(t^m;\nu)\prod_{j=1}^{m-1}\big(1 + \Delta t\, \rho_N^{\mathrm{LB}}(t^j;\nu)\big); \tag{35}$$

we then sum this equation from $m = 1$ to k and recall $e(t^0;\nu) = 0$ to finally arrive at

$$\big(e^k(\nu), e^k(\nu)\big)\prod_{m=1}^{k}\big(1 + \Delta t\, \rho_N^{\mathrm{LB}}(t^m;\nu)\big) \leq \frac{\Delta t}{\nu}\sum_{m=1}^{k}\varepsilon_N^2(t^m;\nu)\prod_{j=1}^{m-1}\big(1 + \Delta t\, \rho_N^{\mathrm{LB}}(t^j;\nu)\big), \quad 1 \leq k \leq K, \tag{36}$$

which is the desired result. □

3.2. Successive Constraint Method

As already indicated, the theory (e.g., *a priori* or even *a posteriori* finite element error analysis) for the Navier-Stokes equations is plagued by exponential growth factors and large prefactors [8,22]. (There are some cases in which algebraic-in-T bounds can be derived [22], however the requisite conditions will not always be satisfied.) The simplest bounds for the exponential growth rate involve the $L^\infty(\Omega)$-norm of the gradient of the velocity — in our case, the gradient of $u_N(t;\nu)$ — which indeed will increase as ν^{-1} as ν decreases. We believe our formulation (26),(19), will improve upon these theoretical estimates — not enough to permit long-time integration at very high Reynolds numbers, but enough to permit practical and rigorous error estimation for (applications characterized by) modest times and modest Reynolds numbers.

There are two reasons for our optimism — admittedly bolstered in hindsight by both the numerical results reported in a later section as well as Navier-Stokes results of subsequent papers [27,26]. First, (19) includes a viscous term that will somewhat constrain the minimizer and hence moderate the minimum: a candidate field large only in a thin destabilizing layer will also incur significant dissipation. Second, $\rho_N(t;\nu)$ of (19) shall be estimated (conservatively but) relatively precisely: our lower bound $\rho_N^{\rm LB}(t;\nu)$ shall reflect the detailed spatial and temporal structure of $u_N(t^k;\nu), 1 \le k \le K$. For the latter calculation we shall adapt the Successive Constraint Method, as we now describe.

The Successive Constraint Method (SCM) introduced in [16,35] is a procedure for the construction of lower bounds for the coercivity and (in the non-coercive case) inf-sup stability constants that appear in reduced basis *a posteriori* error bounds for linear elliptic (and parabolic) PDEs [35]. The SCM — based on an Offline-Online strategy relevant in the many-query and real–time reduced basis context — reduces the Online (real–time/deployed) calculation to a small Linear Program for which the operation count is independent of $\mathcal{N}$. The SCM method can in fact be applied to any generalized eigenproblem: we now consider adaptation to the particular generalized eigenproblem of interest here — our stability constant (19); we empha-

size that the current context is rather more difficult than earlier situations as the underlying eigenproblem (for nonlinear problems) will depend on the reduced basis solution for the field variable.

3.2.1. Preliminaries We first expand the reduced basis solution $u_N^k(\nu)$ as

$$u_N^k(\nu) = \sum_{n=1}^{N} \omega_{N\,n}(t^k;\nu)\xi_n, \tag{37}$$

where $\omega_N(t^k;\nu) = [\omega_{N\,1}(t^k;\nu),\ldots,\omega_{N\,N}(t^k;\nu)]^T \in \boldsymbol{R}^N$ is the reduced basis coefficient vector. We can thus write (19) as

$$\rho_N(t^k;\nu) = \inf_{v\in X^{\mathcal{N}}} \sum_{n=1}^{N+1} \Phi_{N\,n}(t^k;\nu)\frac{d_{N\,n}(v,v)}{\|v\|^2}, \tag{38}$$

where the symmetric bilinear forms $d_{N\,n}$ and the functions $\Phi_{N\,n}(t^k;\nu)$ are given by

$$d_{N\,n}(w,v) = \begin{cases} 2c(\xi_n,w,v) + 2c(\xi_n,v,w), & n = 1,\ldots,N, \\ a(w,v), & n = N+1, \end{cases} \tag{39}$$

and

$$\Phi_{N\,n}(t^k;\nu) = \begin{cases} \omega_{N\,n}(t^k;\nu), & n = 1,\ldots,N, \\ \nu, & n = N+1. \end{cases} \tag{40}$$

It is important to note that the bilinear forms are independent of time and viscosity — this property shall be exploited in our development here.

For clarity of exposition, we introduce a time-parameter quantity $\mu = (t^k;\nu)$ in $\mathcal{D}^\mu \equiv \{t^0,\ldots,t^K\}\times\mathcal{D}$ (recall that $\mathcal{D} \equiv [\nu_{\min},\nu_{\max}]$). We then introduce an objective function $\mathcal{J}_N^{\text{obj}} : \mathcal{D}^\mu \times \mathbb{R}^{N+1} \to \mathbb{R}$ given by

$$\mathcal{J}_N^{\text{obj}}(\mu;y) = \sum_{n=1}^{N+1} \Phi_{N\,n}(\mu)y_n, \tag{41}$$

where $y = [y_1, \ldots, y_{N+1}]^T \in \mathbb{R}^{N+1}$. We may then express our stability constant as

$$\rho_N(\mu) = \inf_{y \in \mathcal{Y}_N} \mathcal{J}_N^{\text{obj}}(\mu; y), \tag{42}$$

where the set $\mathcal{Y}_N \subset \mathbb{R}^{N+1}$ is defined by

$$\mathcal{Y}_N = \left\{ y \in \mathbb{R}^{N+1} \mid \exists w_y \in X^{\mathcal{N}} \text{ s.t. } y_n = \frac{d_{N\,n}(w_y, w_y)}{\|w_y\|^2},\ 1 \le n \le N+1 \right\}. \tag{43}$$

The equivalence between (38) and (42), (43) is readily confirmed.

To construct our lower bound we will replace $\mathcal{Y}_N$ with a set $\mathcal{Y}_N^{\text{LB}} \supset \mathcal{Y}_N$ which leads to easier computation and in particular an Offline-Online decomposition. (We shall also develop an upper bound, which we describe subsequently.) The set $\mathcal{Y}_N^{\text{LB}}$ will contain two types of constraints: "box constraints" that place limits on each element of y independently; and "stability factor constraints" that place limits on linear combinations of the elements of y. We now describe these constraints: in our particular context, both types of constraints are crucial to computational performance.

The box constraints shall take the form $y \in \mathcal{B}_N^{\mathcal{N}}$ for

$$\mathcal{B}_N^{\mathcal{N}} = \prod_{n=1}^{N+1} \left[\underline{\sigma}_{Nn}^{\mathcal{N}}, \overline{\sigma}_{Nn}^{\mathcal{N}} \right], \tag{44}$$

where

$$\underline{\sigma}_{Nn}^{\mathcal{N}} = \inf_{w \in X^{\mathcal{N}}} \frac{d_{N\,n}(w, w)}{\|w\|^2}, \quad \overline{\sigma}_{Nn}^{\mathcal{N}} = \sup_{w \in X^{\mathcal{N}}} \frac{d_{N\,n}(w, w)}{\|w\|^2}, \quad 1 \le n \le N+1. \tag{45}$$

We note that the $d_{N\,n}$ are not bounded with respect to the $L^2(\Omega)$ norm. In general, $|\underline{\sigma}_{Nn}^{\mathcal{N}}|$ (and $|\overline{\sigma}_{Nn}^{\mathcal{N}}|$) $\le \mathcal{N}\|\xi_n\|_X, 1 \le n \le N$, where we recall that $\mathcal{N}$ is the dimension of our truth finite element approximation space. Since in fact $\|\xi_n\|_X \to 0$ exponentially fast as n increases any slight growth with $\mathcal{N}$ is not important or visible in practice. For $n = N+1$, $\underline{\sigma}_{Nn}^{\mathcal{N}}$ is of course bounded and in fact positive as $\mathcal{N} \to \infty$; $\overline{\sigma}_{Nn}^{\mathcal{N}} \to \infty$ as $\mathcal{N} \to \infty$ but plays no role in (42) since $\Phi_{N\,N+1} = \nu > 0$.

The stability factor constraints take the form, for any given μ,

$$\sum_{n=1}^{N+1} \phi_{N\,n}(\mu')y_n > \rho_N(\mu'), \quad \forall \mu' \in \mathcal{C}_J^{M,\mu}. \tag{46}$$

Here $\mathcal{C}_J^{M,\mu}$ is the set of M (≥ 1) points in $\mathcal{C}_J$ closest to the given $\mu \in \mathcal{D}^\mu$, where

$$\mathcal{C}_J \equiv \{\mu_1^{\rm SCM} \in \mathcal{D}^\mu, \ldots, \mu_J^{\rm SCM} \in \mathcal{D}^\mu\}. \tag{47}$$

is an "SCM parameter sample" the construction of which (by a $\text{Greedy}_{\rm SCM}$ procedure) shall be discussed in Section 4.3. Note that we measure proximity in a weighted norm: for $\mu = (t^k; \nu) \in \mathcal{D}^\mu$ and $\mu' = (t^{k'}; \nu') \in \mathcal{C}_J$, the distance between μ and μ' is defined as

$$\text{dist}(\mu, \mu') = \sqrt{(T(\nu - \nu'))^2 + (\nu_{\min}(t^k - t^{k'}))^2}; \tag{48}$$

this choice will ensure that the set $\mathcal{C}_J^{M,\mu}$ contains many points in time near the ν of interest. (Note that if $M > J$, then we set $\mathcal{C}_J^{M,\mu} = \mathcal{C}_J$.) Finally, we denote by

$$\mathcal{R}_{JN} \equiv \{\rho_N(\mu_1^{\rm SCM}), \ldots, \rho_N(\mu_J^{\rm SCM})\} \tag{49}$$

the set of stability factors for the parameter points of the SCM parameter sample $\mathcal{C}_J$.

3.2.2. Lower Bound Now for given $\mathcal{C}_J$, $M \in \mathbb{N} \equiv \{1, 2, \ldots\}$, and any $\mu \in \mathcal{D}^\mu$, we define the "lower bound" set $\mathcal{Y}_N^{\rm LB}(\mu; \mathcal{C}_J, M) \subset \mathbb{R}^{N+1}$ as

$$\mathcal{Y}_N^{\rm LB}(\mu; \mathcal{C}_J, M) \equiv \left\{ y \in \mathbb{R}^{N+1} \mid y \in \mathcal{B}_N^{\mathcal{N}} \,,\, \sum_{n=1}^{N+1} \Phi_{N\,n}(\mu')y_q \geq \rho_N(\mu'), \forall \mu' \in \mathcal{C}_J^{M,\mu} \right\}. \tag{50}$$

We then define our lower bound $\rho_N^{\rm LB}(t^k; \nu) \equiv \rho_N^{\rm LB}(\mu = (t^k; \nu), \mathcal{C}_J, M)$ as

$$\rho_N^{\rm LB}(\mu; \mathcal{C}_J, M) = \min_{y \in \mathcal{Y}_N^{\rm LB}(\mu; \mathcal{C}_J, M)} \mathcal{J}_N^{\rm obj}(\mu; y). \tag{51}$$

We can demonstrate [16,35] that $\mathcal{Y}_N \subset \mathcal{Y}_N^{\rm LB}(\mu; \mathcal{C}_J, M)$ and hence

Proposition 3. *Given $\mathcal{C}_J \subset \mathcal{D}^\mu$ and $M \in \mathbb{N}$,*

$$\rho_N^{\mathrm{LB}}(t^k;\nu) \le \rho_N(t^k;\nu), \quad \forall \mu \equiv (t^k;\nu) \in \mathcal{D}^\mu, \tag{52}$$

for $\rho_N^{\mathrm{LB}}(t^k;\nu) = \rho_N^{\mathrm{LB}}(\mu = (t^k;\nu); \mathcal{C}_J, M)$ defined in (51). □

We note that our lower bound (51) is in fact a linear optimization problem (or Linear Program (LP)). We observe that our LP (51) contains $N+1$ design variables and $2(N+1)+M$ (one-sided) inequality constraints. The crucial observation is that *given* $\mathcal{B}_N^{\mathcal{N}}$ and the sets $\mathcal{C}_J$, and $\mathcal{R}_{JN}$ the operation count to evaluate $\mu \to \rho_N^{\mathrm{LB}}(\mu; \mathcal{C}_J, M)$ is *independent* of $\mathcal{N}$; we discuss the Offline–Online computational implications in the next section.

3.2.3. Upper Bound As we shall see in Section 4.3, we also require an *upper* bound for the stability constant for the (effective) construction of a good SCM parameter sample $\mathcal{C}_J$. For given $\mathcal{C}_J$, $M \in \mathbb{N}$, and any $\mu \in \mathcal{D}^\mu$, we introduce our "upper bound" set $\mathcal{Y}_N^{\mathrm{UB}}(\mu; \mathcal{C}_J, M)$ as

$$\mathcal{Y}_N^{\mathrm{UB}}(\mu; \mathcal{C}_J, M) = \left\{ y^*(\mu') \mid \mu' \in \mathcal{C}_J^{M,\mu} \right\}, \tag{53}$$

where

$$y^*(\mu) = \arg \inf_{y \in \mathcal{Y}_N} \mathcal{J}_N^{\mathrm{obj}}(\mu; y)$$

(in the event of non-uniqueness, any selection criterion suffices). We can then define our upper bound as

$$\rho_N^{\mathrm{UB}}(\mu; \mathcal{C}_J, M) = \min_{y \in \mathcal{Y}_N^{\mathrm{UB}}(\mu; \mathcal{C}_J, M)} \mathcal{J}_N^{\mathrm{obj}}(\mu; y). \tag{54}$$

It directly follows from (53) that $\mathcal{Y}_N^{\mathrm{UB}}(\mu; \mathcal{C}_J, M) \subset \mathcal{Y}_N$ and hence, for given $\mathcal{C}_J$ and $M \in \mathbb{N}$, $\rho_N^{\mathrm{UB}}(\mu; \mathcal{C}_J, M) \ge \rho_N(\mu)$, $\forall\, \mu \in \mathcal{D}^\mu$.

We note that the upper bound (54) is a simple enumeration: *given* the set $\{y^*(\mu') \mid \mu' \in \mathcal{C}_J\}$, the operation count to evaluate $\mu \to \rho_N^{\mathrm{UB}}(\mu; \mathcal{C}_J, M)$ is *independent* of $\mathcal{N}$. We return to the computational implications shortly.

4. Offline–Online Computational Approach

4.1. Construction–Evaluation Decomposition

The calculation of the reduced basis output $s_N(t^k;\nu)$ and output error bound $\Delta_N^s(t^k;\nu)$ admits a Construction–Evaluation decomposition.[1] The expensive — $\mathcal{N}$–dependent — Construction stage, performed once, enables the subsequent very inexpensive — $\mathcal{N}$–independent — Evaluation stage, performed many times for each new desired $\nu \in \mathcal{D}$. Note the reduced basis approach is particularly relevant in the real–time context and the many–query context; for the former the relevant metric is marginal cost — the (inexpensive) Evaluation stage — since the Construction stage is deemed not important; for the latter the relevant metric is asymptotic average cost — again, the (inexpensive) Evaluation stage — since the Construction stage is negligible. We first discuss the Construction–Evaluation approach for $s_N(t^k;\nu), 1 \le k \le K$; we subsequently discuss the Construction–Evaluation approach for the output error bound $\Delta_N^s(t^k;\nu)$.

In order to compute $s_N(t^k;\nu)$ we expand $u_N(t^k;\nu), 1 \le k \le K$, as

$$u_N(t^k;\nu) = \sum_{j=1}^{N} \omega_{N\,j}^k(\nu)\xi_j, \tag{55}$$

where we recall that the $\xi_j, 1 \le j \le N$, are the basis functions for our reduced basis space X_N. We may then evaluate the reduced basis output as

$$s_N(t^k;\nu) = \sum_{j=1}^{N} \omega_{N\,j}^k(\nu)\ell(\xi_j), \quad 1 \le k \le K. \tag{56}$$

It remains to obtain the $\omega_{N\,j}^k(\nu), 1 \le j \le N, 1 \le k \le K$.

[1] This Construction–Evaluation decomposition is essentially the Offline–Online strategy described (in general terms) in the Introduction. However, in the Offline POD-Greedy$_{\text{RB}}$ and Greedy$_{\text{SCM}}$ sampling procedures (described in the next section) we already invoke the Construction–Evaluation decomposition in order to inexpensively evaluate the error bound and stability factor bound, respectively. Hence we use the more precise term Construction–Evaluation — used both in the Offline and Online stages — to describe the procedure by which we can decouple the $\mathcal{N}$–dependent and $\mathcal{N}$–independent components of the basic reduced basis calculations (for the reduced basis coefficients, reduced basis output prediction, stability factor, and *a posteriori* error bounds).

At any given time level t^k, we find $u_N(t^k;\nu)$ from Newton iteration applied to (10): if we denote the current Newton iterate as $\overline{u}_N(t^k;\nu)$ then the Newton increment $\delta u_N(t^k;\nu)$ satisfies

$$\frac{1}{\Delta t}(\delta u_N(t^k;\nu),v) + 2c(\overline{u}_N(t^k;\nu),\delta u_N(t^k;\nu),v) + \nu a(\delta u_N(t^k;\nu),v) = \overline{r}_N(v;t^k;\nu), \quad \forall v \in X_N, \tag{57}$$

where for all $v \in X_N$ (or $X^{\mathcal{N}}$) the Newton residual is given by

$$\begin{aligned}\overline{r}_N(v;t^k;\nu) \equiv f(v) - \frac{1}{\Delta t}(\overline{u}_N(t^k;\nu) - u_N(t^{k-1};\nu),v) \\ - c(\overline{u}_N(t^k;\nu),\overline{u}_N(t^k;\nu),v) - \nu a(\overline{u}_N(t^k;\nu),v).\end{aligned} \tag{58}$$

The next iterate is then given by $\overline{u}_N(t^k;\nu)+\delta u_N(t^k;\nu)$; we continue until convergence. We now express the crucial computational kernel — (57) and (58) — in algebraic form.

Towards that end, we first expand the current Newton iterate and the Newton increment as

$$\overline{u}_N(t^k;\nu) = \sum_{j=1}^{N} \overline{\omega}_{N\,j}^k(\nu)\xi_j, \tag{59}$$

$$\delta u_N(t^k;\nu) = \sum_{j=1}^{N} \delta\omega_{N\,j}^k(\nu)\xi_j, \tag{60}$$

respectively. It then follows from (57) and (58) that the $\delta\omega_{N\,j}^k(\nu), 1 \le j \le N$, satisfy the equations

$$\sum_{j=1}^{N}\left[\frac{\mathcal{M}_{N\,ij}}{\Delta t} + 2\sum_{n=1}^{N}\overline{\omega}_{N\,n}^k(\nu)\mathcal{F}_{N\,nij} + \nu\mathcal{A}_{N\,ij}\right]\delta\omega_{N\,j}^k(\nu) = \overline{r}_N(\xi_i;t^k;\nu), \quad 1 \le i \le N, \tag{61}$$

with

$$\begin{aligned}\overline{r}_N(\xi_i;t^k;\nu) = f(\xi_i) - \sum_{j=1}^{N}\frac{\mathcal{M}_{N\,ij}}{\Delta t}(\overline{\omega}_{N\,j}^k(\nu) - \omega_{N\,j}^{k-1}(\nu)) \\ - \sum_{n=1}^{N}\sum_{j=1}^{N}\mathcal{F}_{N\,nij}\overline{\omega}_{N\,n}^k(\nu)\overline{\omega}_{N\,j}^k(\nu) - \nu\sum_{j=1}^{N}\mathcal{A}_{N\,ij}\overline{\omega}_{N\,j}^k(\nu),\end{aligned} \tag{62}$$

for $1 \le i \le N$. Here the

$$\mathcal{M}_{N\,ij} = (\xi_j, \xi_i), \quad \mathcal{F}_{N\,nij} = c(\xi_n, \xi_j, \xi_i), \quad \mathcal{A}_{N\,ij} = a(\xi_j, \xi_i), \quad 1 \le i, j, n \le N, \tag{63}$$

are parameter–independent arrays. We can now readily identify the Construction–Evaluation decomposition.

In the *Construction* stage we first form and store the time–independent and ν–independent arrays $\mathcal{M}_{N_{\max}\,ij}$, $\mathcal{F}_{N_{\max}\,nij}$, $\mathcal{A}_{N_{\max}\,ij}$, $f(\xi_i)$, and $\ell(\xi_i), 1 \le n, i, j \le N_{\max}$. The operation count in the Construction stage of course depends on $\mathcal{N}$ — even once the $\xi_i, 1 \le i \le N_{\max}$, are *known* (obtained by the $\text{Greedy}_{\text{RB}}$ sampling procedure of the next section), it remains to compute $O(N_{\max}^3)$ finite element quadratures over the triangulation. Note that, thanks to the hierarchical nature of the reduced basis spaces, the stiffness matrices/vectors $\mathcal{M}_{N\,ij}, \mathcal{F}_{N\,nij}, \mathcal{A}_{N\,ij}, f(\xi_i)$, and $\ell(\xi_i), 1 \le n, i, j \le N$, for any $N \le N_{\max}$ can be extracted as principal subarrays of the corresponding $N_{\max}$ quantities. (For non-hierarchical reduced basis spaces the storage requirements are much higher.)

In the *Evaluation* stage, for each Newton iteration at each time level $k = 1, \ldots, K$: we first form the left–hand side of (61) and the residual of (62) — in $O(N^3)$ operations; we then solve the resulting $N \times N$ system of linear equations for $\delta\omega_{N\,j}^k, 1 \le j \le N$ — again in $O(N^3)$ operations (in general, we must anticipate that the reduced basis matrices will be dense). Once the $\omega_{N\,j}^k, 1 \le j \le N, 1 \le k \le K$, are obtained — $O(N^3 K)$ operations in total — we evaluate our output from (56) — in $O(NK)$ operations. The storage and operation count in the Evaluation stage is clearly independent of $\mathcal{N}$, and we can thus anticipate — presuming $N \ll \mathcal{N}$ — very rapid reduced basis response in the real–time and many–query contexts. For problems in higher dimensions the computational savings can be very significant.

We now turn to the error bound $\Delta_N^s(t^k; \nu)$. It is clear from (14) that the output error bound $\Delta_N^s(t^k; \nu)$ can be directly evaluated in terms of the dual norm of ℓ — which we can readily compute in the Construction stage — and the $L^2(\Omega)$ error bound, $\Delta_N^k(\nu)$; we thus

focus on the $L^2(\Omega)$ error bound, $\Delta_N^k(\nu)$. It is furthermore clear from (26) that there are two components to the calculation of $\Delta_N^k(\nu)$: evaluation of $\rho_N^{\rm LB}(t^k;\nu)$ by the Successive Constraint Method, and computation of the dual norm of the residual, $\varepsilon_N(t^k;\nu)$ of (16). We first briefly discuss the Construction–Evaluation decomposition for the former; we then consider the latter (computation of the dual norm for quadratic nonlinearities is described in detail in [36,28], and we thus provide here only a brief summary).

In the Construction stage of the SCM we form the sets $\mathcal{B}_N^{\mathcal{N}}$ and $\mathcal{C}_J, \mathcal{R}_{JN}$ for the lower bound and the set $\{y^*(\mu') \mid \mu' \in \mathcal{C}_J\}$ for the upper bound. Clearly, the operation count for this Construction stage is dependent on $\mathcal{N}$ and quite intensive: we must compute many finite element minimum (and maximum) eigenvalues and associated eigenvectors. In the Evaluation stage of the SCM, both the lower bound and upper bound calculations are quite simple, as already described in Section 3: the lower bound is a small Linear Program; the upper bound is an enumeration/comparison. (In both cases, we must first find the M closest points to μ in $\mathcal{C}_J$ — from (48) — to form $\mathcal{C}_J^{M,\mu}$: this is readily effected by a simple sort.) The storage and operation count in the Evaluation stage is independent of $\mathcal{N}$, and in fact typically quite small relative to other components.

We now turn to the dual norm of the residual. We first note from duality that $\varepsilon_N(t^k;\nu)$ can be expressed as

$$\varepsilon_N^2(t^k;\nu) = \|\hat{e}_N(t^k;\nu)\|_X^2, \quad 1 \le k \le K, \tag{64}$$

where $\hat{e}_N(t^k;\nu)$ is the Riesz representation of the residual,

$$(\hat{e}_N(t^k;\nu), v)_X = r_N(v;t^k;\nu), \quad \forall v \in X^{\mathcal{N}}. \tag{65}$$

Here $r_N(v;t^k;\nu)$ is the residual defined in (17), which we may further write — exploiting the reduced basis representation — as

$$\begin{aligned} r_N(v;t^k;\nu) = f(v) - \frac{1}{\Delta t}\sum_{j=1}^{N}(\omega_{N\,j}^k(\nu) - \omega_{N\,j}^{k-1}(\nu))(\xi_j, v) \\ - \sum_{n=1}^{N}\sum_{j=1}^{N}\omega_{N\,n}^k(\nu)\omega_{N\,j}^k(\nu)c(\xi_n,\xi_j,v) - \nu\sum_{j=1}^{N}\omega_{N\,j}^k(\nu)a(\xi_j,v), \end{aligned} \tag{66}$$

for $1 \le k \le K$.

It now follows directly from (65) and (66) that

$$\hat{e}_N(t^k;\nu) = \sum_{m=1}^{(N+1)^2}\Upsilon_N^m(t^k;\nu)\Gamma_N^m, \quad 1 \le k \le K, \tag{67}$$

where the $\Upsilon_N^m(t^k;\nu)$ depend on timestep and viscosity ν explicitly but also through $\omega(t^k;\nu)$ and $\omega(t^{k-1};\nu)$, and the Γ_N^m are solutions to time–independent and ν–independent "Poisson" problems of the form

$$(\Gamma_N^m, v)_X = g_N^m(v), \quad \forall v \in X^{\mathcal{N}}. \tag{68}$$

The $\Upsilon_N^m(t^k;\nu), g_N^m, 1 \le m \le (N+1)^2$, are given (for a particular ordering) by

$$\begin{aligned} \Upsilon_N^1(t^k;\nu) = 1, \Upsilon_N^2(t^k;\nu) = -\frac{(\omega_{N\,1}^k - \omega_{N\,1}^{k-1})}{\Delta t}, \ldots, \\ \Upsilon_N^{N+2}(t^k;\nu) = -\omega_{N\,1}^k(\nu)\omega_{N\,1}^k(\nu), \ldots, \Upsilon_N^{N^2+2N+1}(t^k;\nu) = -\nu \end{aligned} \tag{69}$$

corresponding to

$$g_N^1(v) = f(v), g_N^2 = (\xi_1, v), \ldots, g_N^{N+2}(v) = c(\xi_1,\xi_1,v)\ldots, g_N^{N^2+2N+1}(v) = a(\xi_N, v). \tag{70}$$

It then follows from (64) that

$$\varepsilon_N^2(t^k;\nu) = \sum_{i=1}^{(N+1)^2}\sum_{j=1}^{(N+1)^2}\Upsilon_N^i(t^k;\nu)\Upsilon_N^j(t^k;\nu)(\Gamma_N^i, \Gamma_N^j)_X, \quad 1 \le k \le K. \tag{71}$$

The Construction–Evaluation decomposition is now clear.

In the *Construction* stage, we find the $\Gamma^m_{N_{\max}}, 1 \le m \le (N_{\max}+1)^2$, and form the inner products $(\Gamma^i_{N_{\max}}, \Gamma^j_{N_{\max}})_X, 1 \le i,j \le (N_{\max}+1)^2$. The operation count for the Construction stage clearly depends on $\mathcal{N}$ — $(N_{\max}+1)^2$ finite element "Poisson" problems (68) and $(N_{\max}+1)^4$ finite element quadratures over the triangulation. (The temporary storage associated with the latter can be excessive for higher–dimensional problems: it is simple to develop procedures that balance temporary storage and re–computation.) Note that, thanks to the hierarchical nature of the reduced basis spaces, the inner products $(\Gamma^i_N, \Gamma^j_N)_X, 1 \le i,j \le (N+1)^2$, for any $N \le N_{\max}$ can be directly extracted from the corresponding $N_{\max}$ quantities. (As already noted, for non-hierarchical reduced basis spaces the storage requirements will be considerably higher.)

In the *Evaluation* stage, given the reduced basis coefficients $\omega_{N\,j}(t^k;\nu), 1 \le j \le N, 1 \le k \le K$: we can readily compute the coefficient functions $\Upsilon^j_N(t^k;\nu), 1 \le j \le (N+1)^2, 1 \le k \le K$; we then simply perform the sum (71) from the stored inner products — $O((N+1)^4)$ operations per time step and hence $O((N+1)^4 K)$ operations in total. As desired, the operation count for the Evaluation stage is indeed independent of $\mathcal{N}$. The quartic scaling with N is obviously less than welcome; however, in actual practice, for modest N the cost to evaluate $s(t^k;\nu)$ and the cost to evaluate $\Delta_N(t^k;\nu)$ are often not too incommensurate — the many $O(N^3)$ operations of the former typically balance the $(N+1)^4$ operations of the latter. Multi-domain (in parameter) approaches can also reduce the deleterious effect of the N^4 scaling.

This concludes the discussion of the Construction–Evaluation decomposition. The Construction stage is performed Offline; the Evaluation stage is invoked Online — for each new ν of interest in the real–time or many–query contexts. However, there are two other components to the Offline stage. First, we must construct a good (rapidly convergent) reduced basis space and associated basis functions $\xi_i, 1 \le i \le N_{\max}$, by a POD-Greedy$_{\rm RB}$ procedure: this sampling process in fact relies on the Construction–Evaluation decomposition to greatly reduce the requisite number of (expensive) "candidate" finite element calculations over an (extensive) Greedy$_{\rm RB}$ training sample, $\Xi_{\rm train,RB}$. And second, we must construct our SCM parameter sample $\mathcal{C}_J$ by a

$\text{Greedy}_{\text{SCM}}$ procedure; this sampling process also relies on the Construction–Evaluation decomposition in particular to greatly reduce the number of (expensive) stability factor calculations over an (extensive) $\text{Greedy}_{\text{SCM}}$ training sample, $\Xi_{\text{train,SCM}}$.

4.2. POD-Greedy$_{\text{RB}}$ Sampling Strategy

We address here the generation of our reduced basis space X_N. Our sampling procedure combines, as first proposed in [15], the POD (Proper Orthogonal Decomposition) in t^k — to capture the causality associated with our evolution equation — with a Greedy procedure [12,38,35] in ν — to treat efficiently the higher dimensions and more extensive ranges of parameter variation. (For an alternative "interpolation" approach to reduced order time-parameter spaces see [1,2].)

To begin, we summarize the well-known optimality property of the POD [24]. Given L elements of $X^{\mathcal{N}}$, $w_j \in X^{\mathcal{N}}, 1 \le j \le L$, and any positive integer $P \le \mathcal{N}$, $\text{POD}(\{w_1, \ldots, w_L\}, P)$ returns P $(\cdot,\cdot)_X$-orthogonal functions $\{\chi_p, 1 \le p \le P\}$ such that the space $V_P = \text{span}\{\chi_p, 1 \le p \le P\}$ is optimal in the sense that

$$V_P = \arg \inf_{Y_P \subset \text{span}\{w_j, 1 \le j \le L\}} \left(\frac{1}{L} \sum_{j=1}^{L} \inf_{v \in Y_P} \|w_j - v\|_X^2 \right)^{1/2},$$

where Y_P denotes a P-dimensional linear space. We also recall that to find the χ_p we first form the correlation matrix C with entries $C_{ij} = (w_i, w_j)_X, 1 \le i, j \le L$; we then find the largest P eigenvalues $\lambda^p, 1 \le p \le P$, and associated eigenvectors $v^p \in \mathbb{R}^L, 1 \le p \le P$, of the system $Cv^p = \lambda^p v^p$ with normalization $(v^p)^T v^p = 1$; finally we form $\chi_p = \sum_{j=1}^{L} v_j^p w_j, 1 \le p \le P$. Note that the χ_p thus satisfy the orthogonality condition $(\chi_m, \chi_n)_X = \lambda^m \delta_{mn}, 1 \le m, n \le P$.

To initiate the $\text{POD-Greedy}_{\text{RB}}$ sampling procedure we must specify a very large (exhaustive) "training" sample of $n_{\text{train,RB}}$ points in $\mathcal{D}$, $\Xi_{\text{train,RB}}$, and an initial (say, random) RB parameter sample $S^* = \{\nu_0^*\}$. Moreover, we shall require a nominal value ρ_N^* for the lower bound of the stability constant: for the purposes of the POD-Greedy sampling *only*, we replace our SCM lower bound with $\rho_N^{\text{LB}}(t^k; \nu) = \rho_N^*, 1 \le k \le K, \forall \nu \in \mathcal{D}$; we then define $\Delta_N^*(t^k; \nu)$ to be our usual

a posteriori L^2 error bound (26) but now with $\rho_N^{\text{LB}}(t^k;\nu)$ replaced by the "nominal" stability factor ρ_N^* — hence $\Delta_N^*(t^k;\nu)$ is not in fact a true error *bound* but rather just an indicator. (We return to this point at the conclusion of this section.)

The algorithm is then given by

`Set` $\mathcal{Z} = \emptyset$;

`Set` $\nu^* = \nu_0^*$;

`While` $N \le N_{\max}$

$\{\chi_p, 1 \le p \le P_1\} = \text{POD}(\{u^{\mathcal{N}}(t^k;\nu^*), 1 \le k \le K\}, P_1)$;

$\mathcal{Z} \leftarrow \{\mathcal{Z}, \{\chi_p, 1 \le p \le P_1\}\}$;

$N \leftarrow N + P_2$;

$\{\xi_n, 1 \le n \le N\} = \text{POD}(\mathcal{Z}, N)$;

$X_N = \text{span}\{\xi_n, 1 \le n \le N\}$;

$\nu^* = \arg\max_{\nu \in \Xi_{\text{train,RB}}} \Delta_N^*(t^K = T;\nu)$

$S^* \leftarrow \{S^*, \nu^*\}$;

`end.`

`Set` $X_N = \text{span}\{\xi_n, 1 \le n \le N\}, 1 \le N \le N_{\max}$.

In actual practice, we typically exit the POD-Greedy sampling procedure at $N = N_{\max} \le N_{\max,0}$ for which a prescribed error tolerance is satisfied: to wit, we define

$$\epsilon_{N,\max}^* = \max_{\nu \in \Xi_{\text{train,RB}}} \Delta_N^*(t^K;\nu),$$

and terminate when $\epsilon_{N,\max}^* \le \epsilon_{\text{tol}}^*$. Note by virtue of the final re–definition the POD-Greedy generates *hierarchical* spaces X_N, $1 \le N \le N_{\max}$, which is computationally very advantageous.

There are two "tuning" variables in the POD-Greedy$_{\rm RB}$ procedure, P_1 and P_2. We choose P_1 to satisfy an internal POD error criterion based on the usual sum of eigenvalues; we choose $P_2 \leq P_1$ to minimize duplication in the reduced basis space — though typically we prefer $P_2 > 1$ in order to reduce the number of Greedy$_{\rm RB}$ iterations and hence Offline cost. We make three observations. First, the POD–Greedy$_{\rm RB}$ method readily accommodates a repeat ν^* in successive Greedy$_{\rm RB}$ cycles — new information will always be available and old information rejected; in contrast, a pure Greedy$_{\rm RB}$ approach in both t and ν [12], though often generating good spaces, can "stall." Second, thanks to the POD normalization $(\chi_m, \chi_n)_X = \lambda^m \delta_{mn}, 1 \leq m, n \leq P_1$, the modes generated in the first POD at any parameter value ν^* are automatically scaled by their respective importance in representing $u(t^k; \nu^*), 1 \leq k \leq K$; the second POD (of $\mathcal{Z}$) is thus correctly weighted to accommodate POD modes from different parameter values. Third, our POD normalization but now in the second POD yields $\|\xi_n\|_X = \sqrt{\lambda^n}, 1 \leq n \leq N_{\max}$, where the λ^n are the eigenvalues of the correlation matrix associated to $\mathcal{Z}$ (of the last Greedy$_{\rm RB}$ iteration); we thus motivate our earlier claims that $\|\xi_n\|_X \to 0$ rapidly as n increases (presuming a rapidly convergent RB approximation) and $\omega^k_{Nn}(\nu) \approx O(1), 1 \leq n \leq N$. The latter are in fact confirmed by our numerical experiments of the next section.

The procedure remains computationally feasible even for large parameter domains and very extensive training samples (and in particular in higher parameter dimensions): the POD is conducted in only one (time) dimension and the Greedy$_{\rm RB}$ addresses the remaining (parameter) dimensions. The crucial point to note is that the operation count for the POD-Greedy$_{\rm RB}$ algorithm is additive and not multiplicative in $n_{\rm train,RB}$ and $\mathcal{N}$: in searching for the next parameter value ν^*, we invoke the Construction–Evaluation decomposition to inexpensively calculate the *a posteriori* error bound at the $n_{\rm train,RB}$ candidate parameter values; in contrast, in a pure POD approach, we would need to evaluate the finite element "truth" solution at the $n_{\rm train,RB}$ candidate parameter values. (Of course, much of the computational economies are due not to the Greedy$_{\rm RB}$ *per se*, but rather to the accommodation within the Greedy$_{\rm RB}$ of the inexpensive

error bounds.) As a result, in the POD-Greedy$_{\rm RB}$ approach we can take $n_{\rm train,RB}$ relatively large: we can thus anticipate reduced basis spaces and approximations that provide rapid convergence *uniformly* over the entire parameter domain. (Note that more sophisticated and hence efficient search algorithms can be exploited in the Greedy$_{\rm RB}$ context, for example [4].)

Once the reduced basis spaces are defined we can then construct our SCM parameter sample, as described in the next section. If we find that the true lower bound is in fact very different from — much more negative than — our nominal value ρ_N^* we may wish to, or need to, return to the POD–Greedy$_{\rm RB}$ algorithm in order to ensure a sufficiently accurate reduced basis approximation. Typically if we choose ρ_N^* and $\epsilon_{\rm tol}^*$ conservatively such a "restart" is not required. It is imperative to note that, in actual Online calculations — evaluations $\mu \rightarrow s_N(t^k;\nu), \Delta_N^{s\,k}(\mu)$ in many–query and real–time applications such as optimization, control, and parameter estimation — we rely on the true stability factor lower bound such that Propositions 2 and 3 are rigorously valid.

4.3. Greedy$_{\rm SCM}$ Sampling Strategy

We now present the construction of the SCM parameter sample $\mathcal{C}_J$ by a Greedy$_{\rm SCM}$ algorithm. We shall require an SCM training sample $\Xi_{\rm train,SCM}$ of $n_{\rm train,SCM}$ points in $\mathcal{D}^\mu$. We also require a tolerance $\epsilon_{\rm SCM}$ of the order of unity which shall control the error in the lower bound prediction.

We first set $J = 1$ and choose $\mathcal{C}_1 = \{\mu_1^{\rm SCM}\}$ "arbitrarily." We then perform

$$\texttt{While} \max_{\mu\in\Xi_{\rm train,SCM}} \left[\frac{\exp(T\,\rho^{\rm UB}_{N_{\rm max}}(\mu;\mathcal{C}_J,M))-\exp(T\,\rho^{\rm LB}_{N_{\rm max}}(\mu;\mathcal{C}_J,M))}{\exp(T\,\rho^{\rm LB}_{N_{\rm max}}(\mu;\mathcal{C}_J,M))}\right] > \epsilon_{\rm SCM}\texttt{:}$$

$$\mu_{J+1}^{\rm SCM} = \arg\max_{\mu\in\Xi_{\rm train,SCM}} \left[\frac{\exp(T\,\rho^{\rm UB}_{N_{\rm max}}(\mu;\mathcal{C}_J,M))-\exp(T\,\rho^{\rm LB}_{N_{\rm max}}(\mu;\mathcal{C}_J,M))}{\exp(T\,\rho^{\rm LB}_{N_{\rm max}}(\mu;\mathcal{C}_J,M))}\right];$$

$$\mathcal{C}_{J+1} = \mathcal{C}_J \cup \mu_{J+1}^{\rm SCM}\ ;$$

$$J \leftarrow J+1\ ;$$

$$\texttt{end.}$$

Note we control not the gap between the upper bound and the lower bound but rather the gap between the exponential of the upper bound and the exponential of the lower bound: this heuristic better reflects the effect of the stability parameter on the ultimate L^2 *a posteriori* error bound. We typically choose $\epsilon_{\text{SCM}} = T\nu_{\max}$.

We denote by $J^{\max}(\epsilon_{\text{SCM}})$ the value of J upon exit — the value of J for which our tolerance is satisfied: our lower bound for $N = N_{\max}$ is thus given by $\rho^{\text{LB}}_{N_{\max}}(t^k;\nu) = \rho^{\text{LB}}_{N_{\max}}(\mu = (t^k;\nu); \mathcal{C}_{J^{\max}}, M)$. It is important to note that our $\text{Greedy}_{\text{SCM}}$ algorithm is performed for $N = N_{\max}$. Then, once the SCM parameter sample has been constructed, we compute the $\rho_N(\mu_j^{\text{SCM}}), 1 \le j \le J^{\max}$ — the $\mathcal{R}_{J^{\max}N}$ — for all $N = 1, \ldots, N_{\max} - 1$. (Note that the $\rho_{N_{\max}}(\mu_j^{\text{SCM}}), 1 \le j \le J^{\max}$ — the $\mathcal{R}_{J^{\max}\,N^{\max}}$ — are already calculated as part of the $\text{Greedy}_{\text{SCM}}$ procedure.) We can thus evaluate $\rho^{\text{LB}}_N(\mu) = \rho^{\text{LB}}_N(\mu; \mathcal{C}_{J^{\max}}, M)$ from (51) — and Proposition 3 remains valid — for any $N \in [1, N_{\max}]$ and any $\mu \in \mathcal{D}^\mu$. Of course, our tolerance ϵ_{SCM} may not be precisely satisfied for all N, and in particular smaller N; however, for the larger N of interest, the greedy selection ensures a sufficiently good lower bound.

Finally, we close by noting that SCM calculation of the nonlinear Burgers' stability factor is particularly demanding: the number of terms in the affine expansion of the objective function increases with N, the dimension of the reduced basis approximation space. (In contrast, for linear problems, the coercivity and inf–sup stability factors depend only on the parametric form of the associated PDE operator.) However, it is important to note that the $\underline{\sigma}^{\mathcal{N}}_{Nn}, \overline{\sigma}^{\mathcal{N}}_{Nn}, 1 \le n \le N$, tend to zero very rapidly as n increases and furthermore $\Phi_{N\,n} = \omega^k_{Nn}(\nu) \approx O(1), 1 \le n \le N$; the variations in, and contributions of, the higher modes are thus tightly controlled — largely mitigating the nominal high dimensionality. As a result, and as we shall observe in Section 5, $J_{\max}$ is relatively small in particular compared to $n_{\text{train,SCM}}$.

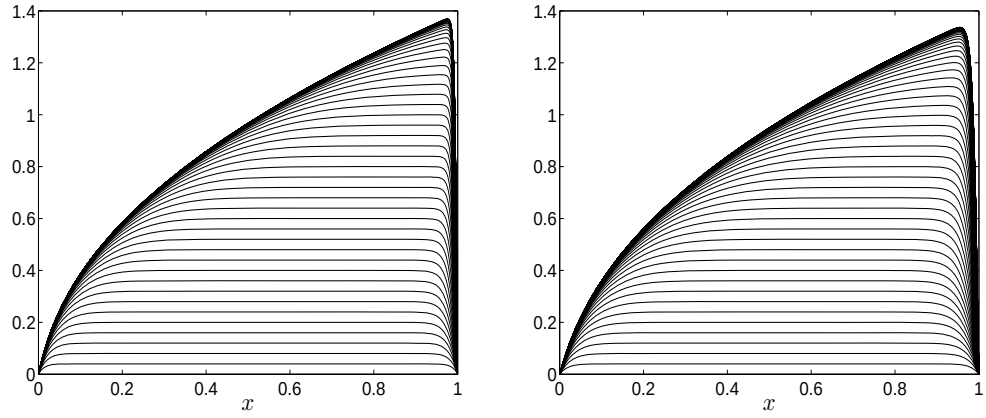

(a) $\nu = 0.005$ (b) $\nu = 0.01$

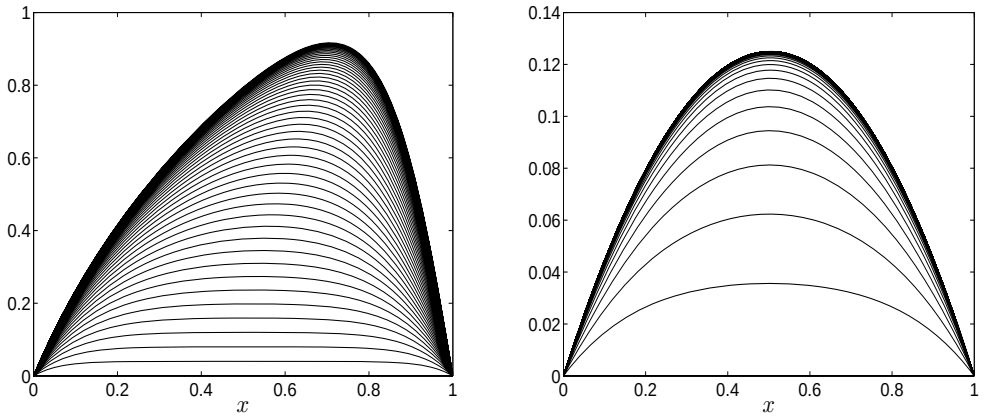

(c) $\nu = 0.1$ (d) $\nu = 1$

Fig. 1. Solution of the Burgers' equation $u^{\mathcal{N}}(x, t^k; \nu)$ as a function of x and t^k: (a) $\nu = 0.005$, (b) $\nu = 0.01$, (c) $\nu = 0.1$, and (d) $\nu = 1$.

5. Numerical Results

We consider the time interval $[0, T]$ with $T = 2$ and viscosity range $\mathcal{D} = [\nu_{\min}, \nu_{\max}]$ with $\nu_{\min} = 0.005$ and $\nu_{\max} = 1$. For the truth approximation we consider a regular mesh of $\mathcal{N} = 201$ degrees of freedom and a constant timestep $\Delta t = 0.02$ corresponding to $K = 100$ timesteps. We present in Figure 1 the truth solution of the time-dependent viscous Burger problem as a function of space and time for $\nu = 1, \nu = 0.1, \nu = 0.01$, and $\nu = 0.005$: the field evolves to a steady state with outer solution $\sim \sqrt{2x}$ and inner boundary layer (at $x = 1$) of thickness ν. (We have confirmed that the results presented in this section are largely insensitive to further increases in $\mathcal{N}$.)

There are of course initial conditions and Burgers' solutions that are more challenging from a reduced basis approximation perspective: in particular, reduced basis spaces are not particularly well suited to the approximation of solutions that exhibit sharp propagating fronts. However, we recall that our analysis of the Burgers' equation is motivated by the incompressible Navier–Stokes equations — for which the "developing boundary layer" Burgers' solution presented here is in fact a more appropriate model problem than a "traveling near shock." In [27,26] we apply the techniques developed in the current paper to fluid flows which exhibit significant boundary layer structure as well as traveling (but incompressible) waves.

We next choose a log uniformly distributed training sample $\Xi_{\text{train,RB}}$ of size $n_{\text{train,RB}} = 50$ and pursue the POD-Greedy$_{\text{RB}}$ sampling procedure with $\rho_N^* = 0$, $\nu_0^* = 0.005$, and $\epsilon_{\text{tol}}^* = 10^{-3}$. The POD-Greedy$_{\text{RB}}$ sampling procedure terminates after 6 POD–Greedy iterations — one iteration is defined as one pass through the `While` loop — and yields $N_{\max} = 17$ and the optimal RB parameter sample

$$S^* = [0.0050, 0.0365, 0.0107, 0.1424, 0.0057, 0.0065, 0.0074].$$

We observe, not surprisingly, that most of the POD–Greedy$_{\text{RB}}$ sample points are close to $\nu_{\min} = 0.005$. We present in Figure 2 $\epsilon_{N,\max}^*$ as a function of POD-Greedy$_{\text{RB}}$ iteration number (and N). Clearly, the error indicator $\epsilon_{N,\max}^*$ decreases very rapidly with N; we shall subsequently confirm that the rigorous error bound, and hence also the true error, also decreases very rapidly with N.

We now turn to the stability factor. Given the Greedy$_{\text{SCM}}$ training sample $\Xi_{\text{train,SCM}} = \{t^2, t^4, \ldots, t^K\} \times \Xi_{\text{train,RB}}$ we perform the Greedy$_{\text{SCM}}$ procedure of Section 4.3 to construct the lower bound for the stability factor. We present in Figure 3 the SCM parameter sample $\mathcal{C}_J$ for $J = J^{\max} = 80$; we observe that most of the sample points are close to $\nu_{\min} = 0.005$, and that many sample points correspond to the final time $T = 2$. Note that $J^{\max}$ is *much less* than $n_{\text{train,SCM}}$ and hence the SCM is clearly providing substantial approximation in (discrete)

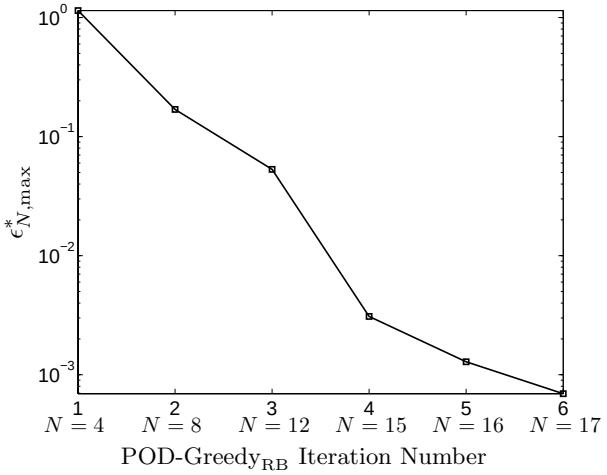

Fig. 2. The error indicator $\epsilon^*_{N,\max}$ as a function of POD-Greedy iteration number and also N.

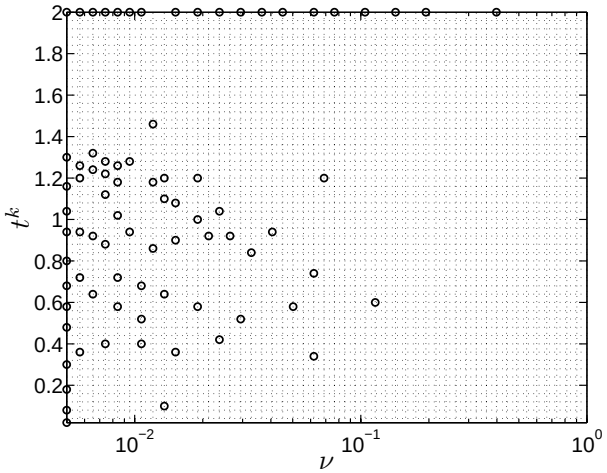

Fig. 3. Distribution of the SCM parameter sample $\mathcal{C}_J$ in time (linear scale) and parameter (log scale). The grid represents $\Xi_{\mathrm{train,SCM}}$: each horizontal gray line corresponds to a $t^k, k = 2, 4, ..., K$; each vertical gray line corresponds to a point in $\Xi_{\mathrm{train,RB}}$.

time and (continuous) parameter. The (POD–Greedy$_{\mathrm{RB}}$) reduced basis approximation $u_N(t^k;\nu)$ will converge much more rapidly to $u^{\mathcal{N}}(t^k;\nu)$ in N than the (Greedy$_{\mathrm{SCM}}$) SCM approximation $\rho_N^{LB}(t^k;\nu)$ will converge to $\rho_N(t^k;\nu)$ in J: the reduced basis projection exploits smoothness in parameter and Galerkin optimality, whereas the SCM construction — focused on a lower bound — enlists only rather weak constraints and (implicitly) low–order interpolation. Fortunately, whereas we require a highly accurate reduced basis approximation, we are content with a relatively crude stability factor; note also that whereas the reduced basis Online operation count depends on N, the SCM Online operation count depends on M — here $M = 16$ — and not $J^{\max}$.

We now present in Figure 4 the stability factor $\rho_N(t^k;\nu)$ as a function of t^k for $\nu = 1, 0.1, 0.01,$ and 0.005 for $N = 17$; we also present the stability factor lower bound $\rho_N^{\rm LB}(t^k;\nu)$ as well as the corresponding upper bound $\rho_N^{\rm UB}(t^k;\nu)$. As already indicated, $\rho_N(t^k;\nu)$ reflects the detailed spatial and temporal structure of $u_N^k(\nu), 1 \le k \le K$, as well as viscous stabilization effects. As a result, even for $\nu = 0.005$ — clearly a convectively–dominated highly nonlinear flow — $\rho_N(t^k;\nu)$ is still mostly positive (stable): in our particular example, $u_N^k(\nu)$ is "dangerous" only within the boundary layer. It should also be noted that the SCM yields a very good upper bound for the stability factor (this SCM upper bound is also significantly less complicated and less costly than a standard reduced basis Rayleigh–Ritz aproximation): the difference between $\rho_N^{\rm UB}(t^k;\nu)$ and $\rho_N(t^k;\nu)$ is indeed very small. (If we replace $\rho_N^{\rm LB}(t^k;\nu)$ with $\rho_N^{\rm UB}(t^k;\nu)$ in (26) we will certainly obtain better error bounds — but we can no longer provide rigorous guarantees.)

Finally, we present in Figure 5 the actual $L^2(\Omega)$ error, $\|u^{\mathcal{N}}(\cdot,t^k;\nu) - u_N(\cdot,t^k;\nu)\|$, and the error bound, $\Delta_N(t^k;\nu)$, as a function of discrete time t^k for $N = 5, 10,$ and 15 and for $\nu = 0.005, 0.01, 0.1,$ and 1. Figure 6 provides the output error, $|s^{\mathcal{N}}(t^k;\nu) - s_N(t^k;\nu)|$, and the output error bound, $\Delta_N^s(t^k;\nu)$, for the same values of N and ν. We observe that the reduced basis approximation converges quite rapidly, and that furthermore the *a posteriori* error bound $\Delta_N(t^k;\nu)$ is (rigorous, but also) reasonably sharp; indeed, even for $\nu = 0.005$, the numerical approximation and associated *a posteriori* error estimators are both still quite good for times of order unity. However, the output error bound $\Delta_N^s(t^k;\nu)$ is not as sharp as the L^2 error bound $\Delta_N(t^k;\nu)$: the output effectivity $\eta_N^s(t^k;\nu)$ can be as large as $O(1000)$, whereas the L^2 effectivity $\eta_N(t^k;\nu)$ is only $O(10)$; we believe that the sharpness of the output error bound can be significantly improved by introduction of adjoint techniques [22,29] — this development will be pursued in future work.

In summary, for ν very small — Reynolds number very large — and for large final times T our *a posteriori* error bounds *will certainly no longer be useful*. However, our initial calculations for the full incompressible Navier–Stokes equations [27,26] indicate that our methods can in fact

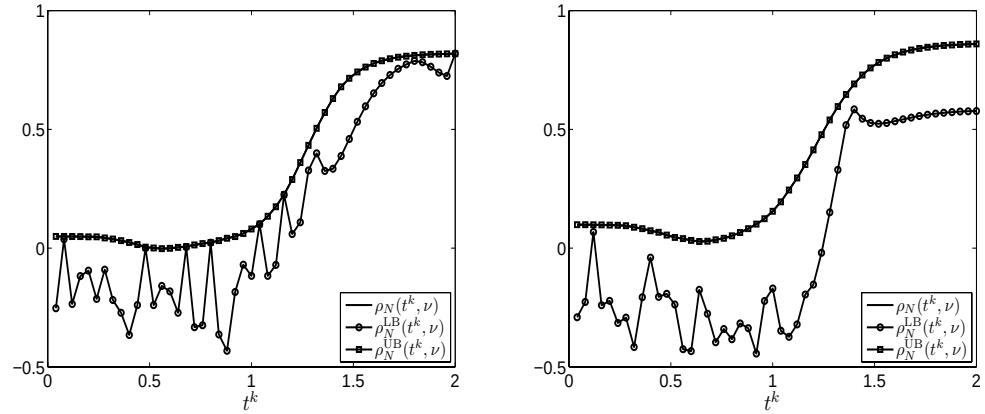

(a) $\nu = 0.005$ (b) $\nu = 0.01$

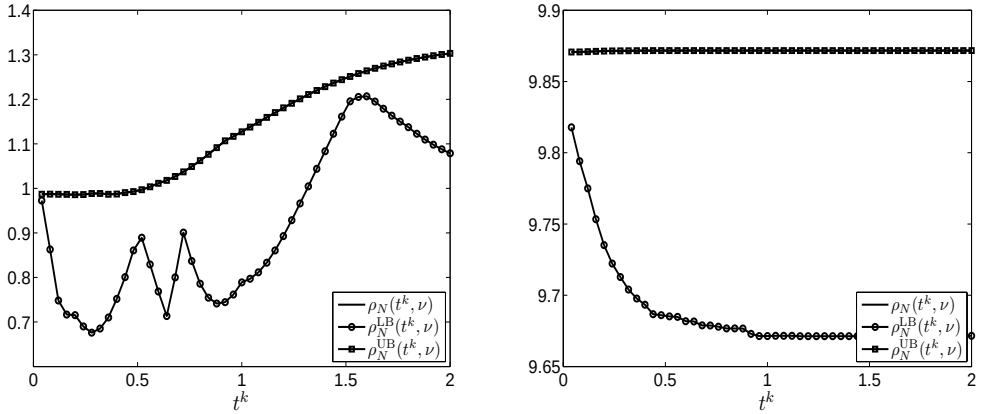

(c) $\nu = 0.1$ (d) $\nu = 1$

Fig. 4. Stability factors $\rho_N(t^k;\nu)$, $\rho_N^{\mathrm{LB}}(t^k;\nu)$, and $\rho_N^{\mathrm{UB}}(t^k;\nu)$ as a function of t^k for $N = 17$: (a) $\nu = 0.005$, (b) $\nu = 0.01$, (c) $\nu = 0.1$, and (d) $\nu = 1$.

treat problems relevant to engineering and science — for example, complex flow bifurcations: we obtain certified accuracies of 1%–5% at greatly reduced (Online) cost relative to classical finite element approaches.

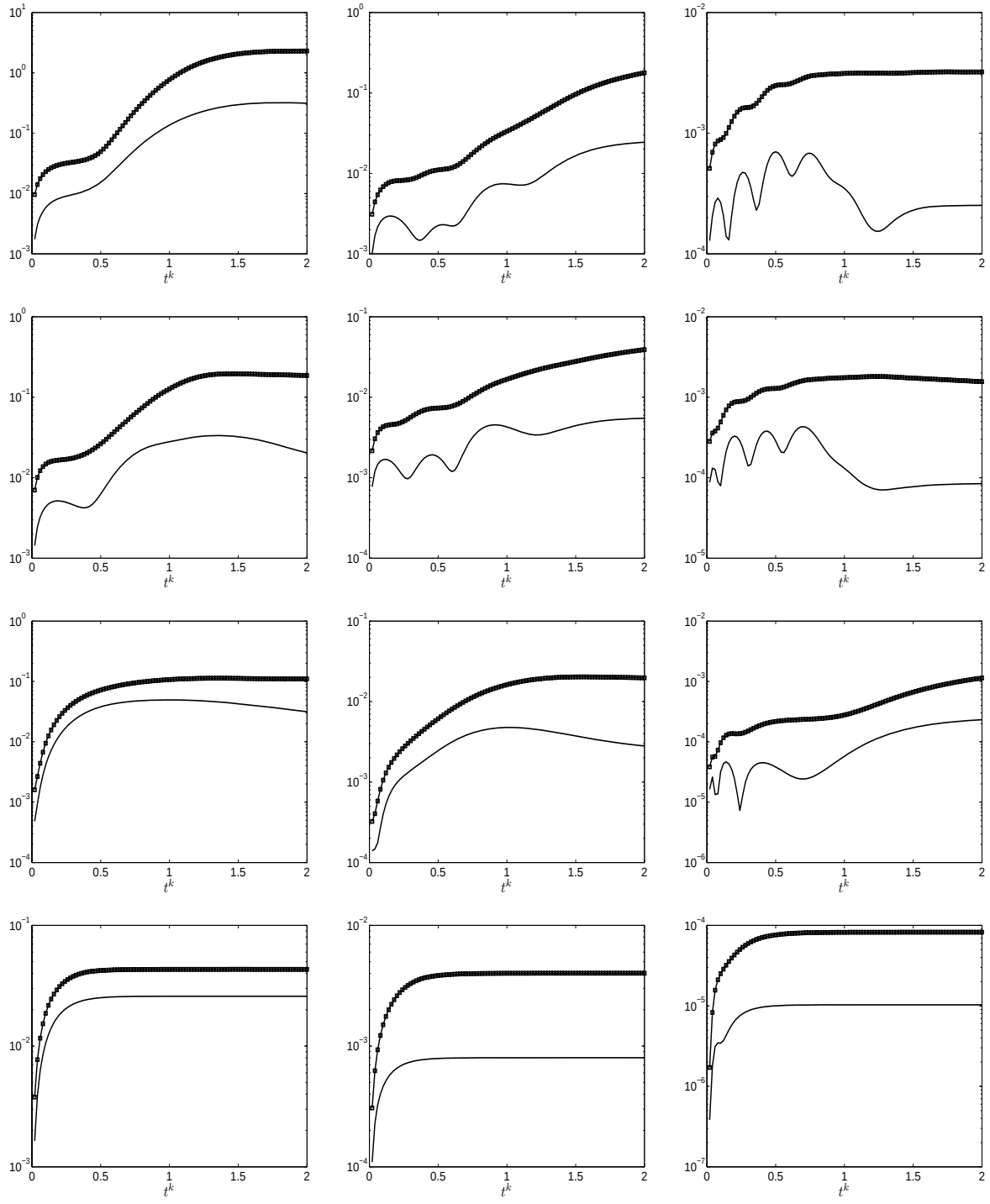

Fig. 5. The actual $L^2(\Omega)$ error, $\|u^{\mathcal{N}\,k}(\nu) - u_N^k(\nu)\|$ (solid line), and the L^2 error bound, $\Delta_N^k(\nu)$ (square symbol), as a function of discrete time t^k for $N = 5$ (first column), 10 (second column), and 15 (third column) and for $\nu = 0.005$ (top row), $\nu = 0.01$ (second row), $\nu = 0.1$ (third row), and $\nu = 1$ (bottom row).

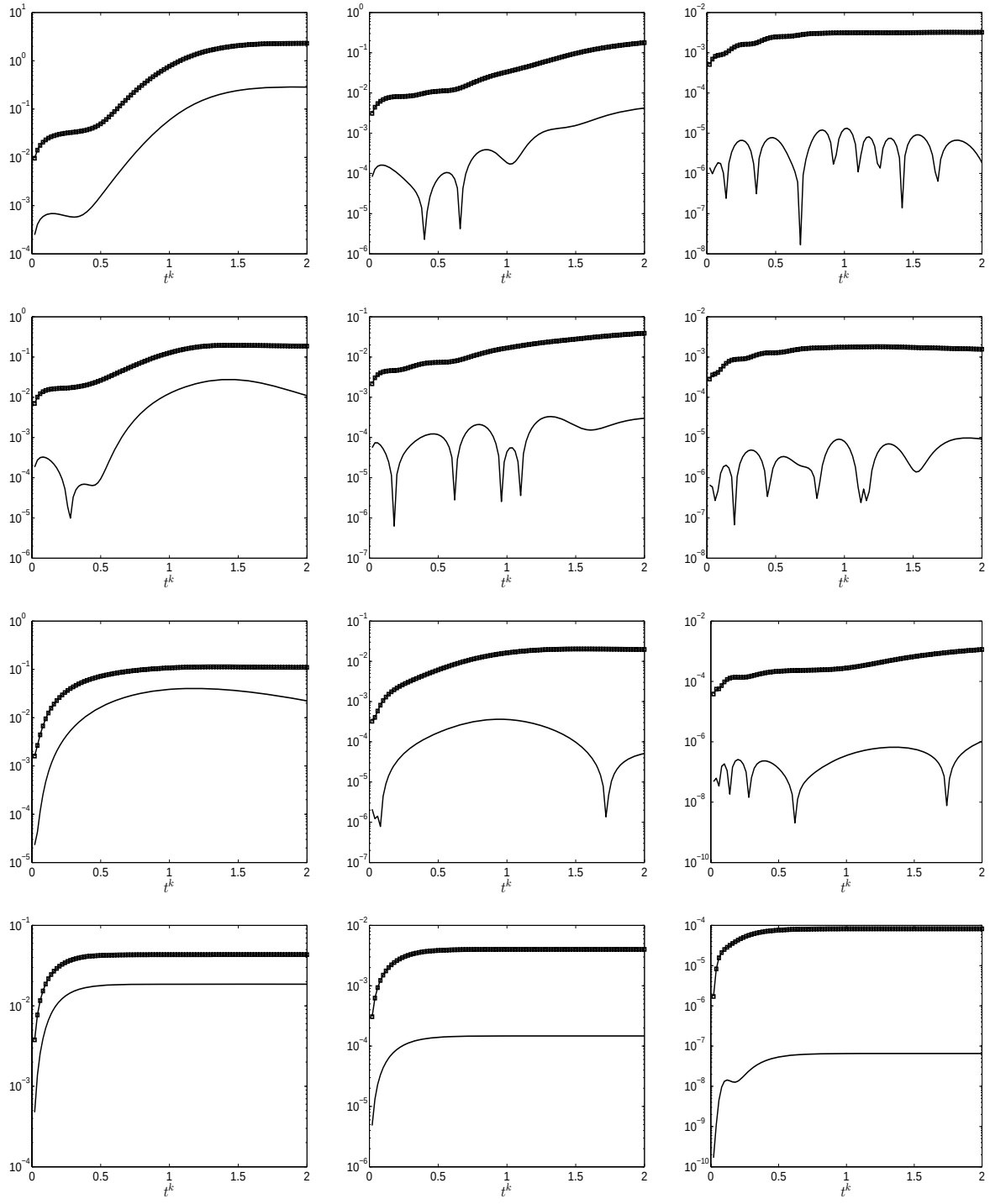

Fig. 6. The output error, $|s^{\mathcal{N}\,k}(\nu) - s_N^k(\nu)|$ (solid line), and the output error bound, $\Delta_N^{s\,k}(\nu)$ (square symbol), as a function of discrete time t^k for $N = 5$ (first column), 10 (second column), and 15 (third column) and for $\nu = 0.005$ (top row), $\nu = 0.01$ (second row), $\nu = 0.1$ (third row), and $\nu = 1$ (bottom row).

References

1. Amsallem, D., Cortial, J., Farhat, C.: On-demand CFD-based aeroelastic predictions using a database of reduced-order bases and models. In: 47th AIAA Aerospace Sciences Meeting, 5 - 8 January 2009, Orlando, Florida (2009). Paper 2009-800
2. Amsallem, D., Farhat, C.: Interpolation method for adapting reduced-order models and application to aeroelasticity. AIAA Journal **46**(7), 1803–1813 (2008)
3. Barrault, M., Nguyen, N.C., Maday, Y., Patera, A.T.: An "empirical interpolation" method: Application to efficient reduced-basis discretization of partial differential equations. C. R. Acad. Sci. Paris, Série I. **339**, 667–672 (2004)
4. Bui-Thanh, T., Willcox, K., Ghattas, O.: Model reduction for large-scale systems with high-dimensional parametric input space (AIAA Paper 2007-2049). In: Proceedings of the 48th AIAA/ASME/ASCE/AHS/ASC Structures, Structural Dynamics and Material Conference (2007)
5. Burkardt, J., Gunzburger, M.D., Lee, H.C.: Pod and cvt-based reduced order modeling of Navier-Stokes flows. Comp. Meth. Applied Mech. **196**, 337–355 (2006)
6. Cancès, E., Le Bris, C., Nguyen, N.C., Maday, Y., Patera, A.T., Pau, G.S.H.: Feasibility and competitiveness of a reduced basis approach for rapid electronic structure calculations in quantum chemistry. In: Proceedings of the Workshop for High-dimensional Partial Differential Equations in Science and Engineering (Montreal), vol. 41, pp. 15–57 (2007)
7. Christensen, E.A., Brons, M., Sorensen, J.N.: Evaluation of pod-based decomposition techniques applied to parameter-dependent non-turbulent flows. SIAM J. Sci. Comput. **21**, 1419 (2000)
8. Constantin, P., Foias, C.: Navier-Stokes Equations. Chicago Lectures in Mathematics. University of Chicago Press, Chicago, IL (1988)
9. Deane, A., Kevrekidis, I., Karniadakis, G., Orszag, S.: Low-dimensional models for complex geometry flows: Application to grooved channels and circular cylinders. Phys. Fluids **10**, 2337–2354 (1991)
10. Grepl, M.: Reduced-basis approximations and *a posteriori* error estimation for parabolic partial differential equations. Ph.D. thesis, Massachusetts Institute of Technology (2005)
11. Grepl, M.A., Maday, Y., Nguyen, N.C., Patera, A.T.: Efficient reduced-basis treatment of nonaffine and nonlinear partial differential equations. M2AN (Math. Model. Numer. Anal.) **41**(2), 575–605 (2007)
12. Grepl, M.A., Patera, A.T.: *A Posteriori* error bounds for reduced-basis approximations of parametrized parabolic partial differential equations. M2AN (Math. Model. Numer. Anal.) **39**(1), 157–181 (2005)
13. Gunzburger, M.D.: Finite Element Methods for Viscous Incompressible Flows. Academic Press (1989)

14. Gunzburger, M.D., Peterson, J., Shadid, J.N.: Reduced-order modeling of time-dependent PDEs with multiple parameters in the boundary data. Comp. Meth. Applied Mech. **196**, 1030–1047 (2007)
15. Haasdonk, B., Ohlberger, M.: Reduced basis method for finite volume approximations of parametrized linear evolution equations. Mathematical Modelling and Numerical Analysis (M2AN) **42**(3), 277–302 (2008)
16. Huynh, D.B.P., Rozza, G., Sen, S., Patera, A.T.: A successive constraint linear optimization method for lower bounds of parametric coercivity and inf-sup stability constants. C. R. Acad. Sci. Paris, Analyse Numérique (2007)
17. Ito, K., Ravindran, S.S.: A reduced basis method for control problems governed by PDEs. In: W. Desch, F. Kappel, K. Kunisch (eds.) Control and Estimation of Distributed Parameter Systems, pp. 153–168. Birkhäuser (1998)
18. Ito, K., Ravindran, S.S.: A reduced-order method for simulation and control of fluid flows. Journal of Computational Physics **143**(2), 403–425 (1998)
19. Ito, K., Ravindran, S.S.: Reduced basis method for optimal control of unsteady viscous flows. International Journal of Computational Fluid Dynamics **15**(2), 97–113 (2001)
20. Ito, K., Schroeter, J.D.: Reduced order feedback synthesis for viscous incompressible flows. Mathematical And Computer Modelling **33**(1-3), 173–192 (2001)
21. Johansson, P.S., Andersson, H., Rønquist, E.: Reduced-basis modeling of turbulent plane channel flow. Computers and Fluids **35**(2), 189–207 (2006)
22. Johnson, C., Rannacher, R., Boman, M.: Numerical and hydrodynamic stability: Towards error control in computational fluid dynamics. SIAM Journal of Numerical Analysis **32**(4), 1058–1079 (1995)
23. Joseph, D.: Stability of fluid motions. I. & II., *Springer Tracts in Natural Philosophy*, vol. 27 & 28. Springer-Verlag, New York (1976)
24. Kunisch, K., Volkwein, S.: Galerkin proper orthogonal decomposition methods for a general equation in fluid dynamics. SIAM J. Num. Analysis **40**(2), 492–515 (2002)
25. LeVeque, R.J.: Numerical Methods for Conservation Laws. Lectures in Mathematics, ETH-Zurich. Birkhauser-Verlag, Basel (1990)
26. Nguyen, N.C., Patera, A.T.: Reduced basis approximation and a posteriori error estimation for the parametrized unsteady Boussinesq equations; application to natural convection in a laterally heated cavity. Journal of Computational Physics (2009). Submitted.
27. Nguyen, N.C., Rozza, G., Huynh, D.B.P., Patera, A.T.: Reduced basis approximation and a posteriori error estimation for parametrized parabolic PDEs; application to real-time Bayesian parameter estimation.

In: L. Biegler, G. Biros, O. Ghattas, M. Heinkenschlos, D. Keyes, B. Mallick, L. Tenorio, B. van Bloemen Waanders, K. Willcox (eds.) Computational Methods for Large Scale Inverse Problems and Uncertainty Quantification. John Wiley and Sons, UK. Submitted.

28. Nguyen, N.C., Veroy, K., Patera, A.T.: Certified real-time solution of parametrized partial differential equations. In: S. Yip (ed.) Handbook of Materials Modeling, pp. 1523–1558. Springer (2005)
29. Pierce, N., Giles, M.B.: Adjoint recovery of superconvergent functionals from PDE approximations. SIAM Review **42**(2), 247–264 (2000)
30. Porsching, T.A., Lee, M.Y.L.: The reduced-basis method for initial value problems. SIAM Journal of Numerical Analysis **24**, 1277–1287 (1987)
31. Prud'homme, C., Rovas, D., Veroy, K., Maday, Y., Patera, A., Turinici, G.: Reliable real-time solution of parametrized partial differential equations: Reduced-basis output bounds methods. Journal of Fluids Engineering **124**(1), 70–80 (2002)
32. Quarteroni, A., Rozza, G.: Numerical solution of parametrized Navier-Stokes equations by reduced basis method. Num. Meth. PDEs **23**, 923–948 (2007)
33. Quarteroni, A., Valli, A.: Numerical Approximation of Partial Differential Equations, 2nd edn. Springer (1997)
34. Rovas, D., Machiels, L., Maday, Y.: Reduced basis output bounds methods for parabolic problems. IMA J. Appl. Math. **26**, 423–445 (2006)
35. Rozza, G., Huynh, D., Patera, A.: Reduced basis approximation and a posteriori error estimation for affinely parametrized elliptic coercive partial differential equations — application to transport and continuum mechanics. Arch. Comput. Methods Eng. **15**(3), 229–275 (2008)
36. Veroy, K., Patera, A.T.: Certified real-time solution of the parametrized steady incompressible Navier-Stokes equations; Rigorous reduced-basis *a posteriori* error bounds. International Journal for Numerical Methods in Fluids **47**, 773–788 (2005)
37. Veroy, K., Prud'homme, C., Patera, A.T.: Reduced-basis approximation of the viscous Burgers' equation: Rigorous *a posteriori* error bounds. C. R. Acad. Sci. Paris, Série I **337**(9), 619–624 (2003)
38. Veroy, K., Prud'homme, C., Rovas, D.V., Patera, A.T.: *A Posteriori* error bounds for reduced-basis approximation of parametrized noncoercive and nonlinear elliptic partial differential equations. In: Proceedings of the 16th AIAA Computational Fluid Dynamics Conference (2003). Paper 2003-3847